

# Distributed Signal Processing for Extremely Large-Scale Antenna Array Systems: State-of-the-Art and Future Directions

Yanqing Xu, *Member, IEEE*, Erik G. Larsson, *Fellow, IEEE*, Eduard A. Jorswieck, *Fellow, IEEE*, Xiao Li, *Senior Member, IEEE*, Shi Jin, *Fellow, IEEE*, and Tsung-Hui Chang, *Fellow, IEEE*

**Abstract**—Extremely large-scale antenna arrays (ELAA) play a critical role in enabling the functionalities of next generation wireless communication systems. However, as the number of antennas increases, ELAA systems face significant bottlenecks, such as excessive interconnection costs and high computational complexity. Efficient distributed signal processing (SP) algorithms show great promise in overcoming these challenges. In this paper, we provide a comprehensive overview of distributed SP algorithms for ELAA systems, tailored to address these bottlenecks. We start by presenting three representative forms of ELAA systems: single-base station ELAA systems, coordinated distributed antenna systems, and ELAA systems integrated with emerging technologies. For each form, we review the associated distributed SP algorithms in the literature. Additionally, we outline several important future research directions that are essential for improving the performance and practicality of ELAA systems.

**Index Terms**—Extremely large-scale antenna array, decentralized baseband processing, distributed antenna system, distributed signal processing

## I. INTRODUCTION

### A. Multi-Antenna-Enabled Wireless Communications

Wireless communications have undergone remarkable development over the past few decades, driven by numerous technological advancements. Innovations such as new air interfaces for accelerated data transmission, advanced source and channel coding for improved efficiency and reliability, and streamlined protocols to minimize overheads have played pivotal roles. During this journey, the invention of multi-antenna techniques stands out as one of the most significant milestones. In multi-antenna-enabled wireless communications, systems deploy multiple antennas at the transmitter, the

receiver, or both ends, allowing the exploitation of additional spatial degrees of freedom. This provides substantial benefits across three key areas: spatial diversity, spatial multiplexing, and beamforming gain [1]. By harnessing these capabilities, multi-antenna technology substantially boosts spectral and energy efficiency, enhances link reliability, and delivers these improvements without the need for additional spectrum [2]–[5].

Multi-antenna techniques have been successfully used in modern wireless communication systems, enhancing both commercial and private networks worldwide. In mobile telecommunications, these technologies are essential for 4G long-term evolution (LTE), 5G new radio (NR), and the upcoming 6G networks, facilitating substantial increases in data rates and network capacity while significantly reducing latency [6]. Additionally, multi-antenna systems play a vital role in Wi-Fi technology, from the 802.11n standard to the latest 802.11ax (Wi-Fi 6), by supporting multi-user multiple-input multiple-output (MU-MIMO) [7], [8]. This capability allows routers to communicate with multiple devices simultaneously at the same radio resource, improving network throughput and reducing latency in multi-device environments. Beyond terrestrial networks, multi-antenna techniques are also critical in satellite communications, where the link robustness and capacity can be enhanced by directing signals more precisely towards specific areas on Earth through advanced beamforming capabilities [9]–[11]. Moreover, these antenna technologies are instrumental in specialized applications such as radar and navigation systems used in the aerospace and maritime sectors, enhancing safety in autonomous vehicles and aircraft systems [12], [13].

### B. Evolution of Multi-Antenna Techniques

The benefits of using multiple antennas for communication were observed at the very early stages of wireless communications [14]. However, the beamforming gains and spatial diversity offered by multiple antennas were not thoroughly understood until 1998 [15], which theoretically demonstrated that MIMO systems could potentially increase the capacity of a wireless point-to-point link linearly with the number of antennas at the transmitter and receiver, without the need for additional power or bandwidth. Subsequently, numerous fundamental contributions have been made by the research community to understand the performance limits of MIMO-

T.-H. Chang is the corresponding author.

Y. Xu, and T.-H. Chang are with the School of Science and Engineering, The Chinese University of Hong Kong, Shenzhen, and also with the Shenzhen Research Institute of Big Data, Shenzhen 518172, China (e-mail: xuyanqing@cuhk.edu.cn, tsunghui.chang@ieee.org).

E. G. Larsson is with the Department of Electrical Engineering (ISY), Linköping University, 581 83 Linköping, Sweden (e-mail: erik.g.larsson@liu.se).

E. A. Jorswieck is with the Institute for Communications Technology, Technical University of Braunschweig, 38106 Braunschweig, Germany (e-mail: e.jorswieck@tu-braunschweig.de).

X. Li, and S. Jin are with the National Mobile Communication Research Laboratory, Southeast University, Nanjing 210096, China (e-mail: li\_xiao, jinshi@seu.edu.cn).

This work has been submitted to the IEEE for possible publication. Copyright may be transferred without notice, after which this version may no longer be accessible.

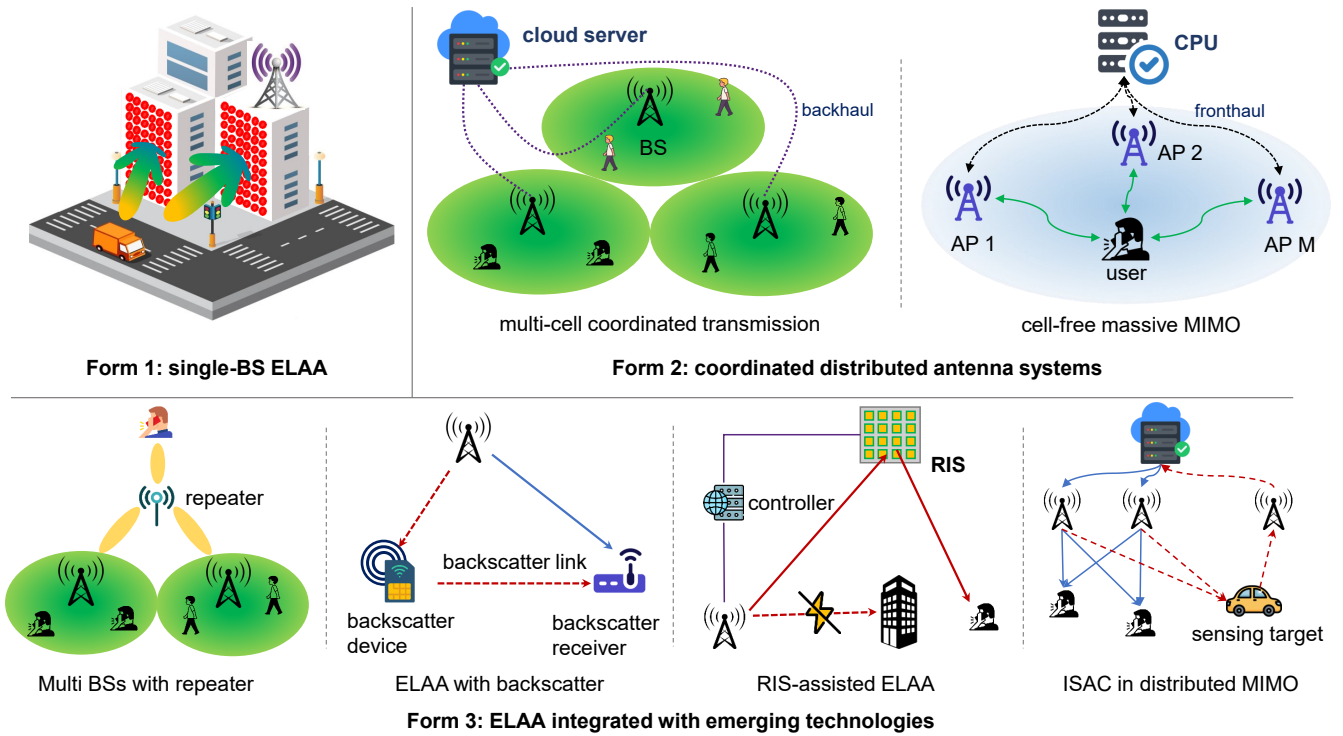


Fig. 1: Illustrations of representative forms of ELAA systems (top row) and four strategies with relevant technologies (bottom row).

based systems [16]–[24]. Among these, the work [16] characterized the capacity of multi-antenna channels under Gaussian channels, while the work [17] extended these findings to more realistic fading channels. A simple space-time coding technique was introduced in [18] which enabled transmit diversity and laid the foundation for later MIMO developments. Additionally, the trade-off between diversity gain and multiplexing gain in MIMO systems was explored in [19]. Parallel to these academic advancements, MIMO technology was prepared for practical application through standardization efforts by the 3rd generation partnership project (3GPP) [25]–[28]. Thanks to these theoretical contributions from the research community and successful standardization, MIMO became one of the most important enabling technologies in 4G LTE systems.

As an advancement of the MIMO technique, the concept of massive MIMO was introduced in [29]. In massive MIMO systems, the number of antennas at the base station (BS) scales up by orders of magnitude compared to traditional MIMO systems; for example, configurations include 64 or more antennas [2], [30]–[32]. Owing to the massive number of antennas, these systems can leverage spatial multiplexing to a much greater extent than was previously possible, thereby achieving unprecedented improvements in throughput and efficiency. Research indicates that by increasing the number of antennas, massive MIMO systems using simple linear processing techniques such as zero-forcing (ZF) and matched filtering (MF) can achieve compelling spectral and energy efficiency [33], [34]. This shift not only reduces the complexity but also increases the robustness of wireless networks against fading and other channel impairments. Due to these advantages, massive MIMO serves as a fundamental enabling technique

in 5G NR to support enhanced mobile broadband, massive machine-type communication, as well as ultra-reliable and low-latency communication [35]–[39].

As we transition into the 6G era, wireless systems are set to deliver enhanced performance to enable much more sophisticated applications such as immersive communication, massive communication, and hyper reliable and low-latency communication, as defined by the International Telecommunication Union Radiocommunication Sector (ITU-R) [40]. Within this framework, multi-antenna technologies continue to serve as a cornerstone, evolving into increasingly advanced systems to meet these ambitious goals. To achieve higher data rates, lower latency, and greater connectivity envisioned for 6G, there is a pressing need to advance antenna technologies by further increasing the number of antennas. This has led to the emergence of extremely large-scale antenna array (ELAA) systems<sup>1</sup>. The increase in the number of antennas can be achieved through two approaches: by augmenting the number of antennas at a single transmitter or by coordinating multiple transmitters for joint transmissions [44]–[48].

With an extremely large number of antennas, ELAA systems offer significant advantages over conventional antenna configurations, including enhanced spatial resolution, better wireless channel sounding, and improved power efficiency, making them a promising solution for addressing the challenges of next-generation networks. The importance of ELAA as a critical enabling technology for next-generation networks has also been evidenced by industrial initiatives from leading telecom

<sup>1</sup>For some application scenarios, such as satellite communications, where adaptability and massive connectivities are not critical, one can use reflector-arrays as a cost-effective approach to create large-scale antenna array systems [41]–[43].

companies. For instance, Nokia and AT&T collaborated to demonstrate that the cooperative distributed massive MIMO system can increase the uplink capacity between 60% and 90% compared to similarly configured systems with a single panel, without sacrificing the downlink performance [49], and Huawei has also successfully deployed distributed massive MIMO systems in indoor cellular networks [50].

### C. Features and Challenges of ELAA Systems

ELAA systems can take various forms, each tailored to enhance wireless network performance through advanced antenna technologies. In this paper, we particularly focus on three representative forms of ELAA systems, as shown in Fig. 1. The first form is the single-BS ELAA system, characterized by an extremely large number of antennas at a single BS. The second form involves coordinating a large number of distributed antennas across multiple sites for joint transmission. This approach leverages spatial diversity to a greater extent, enhancing coverage and reducing signal fading and interference across large areas. The third form integrates ELAA systems with emerging technologies, such as network-controlled repeaters, reconfigurable intelligent surfaces (RIS), and wireless sensing nodes. These technologies introduce additional flexibility and functionality, enabling ELAA systems to adapt more effectively to dynamic environmental conditions and user demands, thereby opening new avenues for network optimization and service delivery.

The deployment of ELAA systems, while offering substantial benefits, also introduces significant challenges due to the extremely large number of antennas involved, including 1) excessive interconnection cost between the antennas and baseband processor to collect the received signals for processing, 2) high computational complexity due to large-scale signal processing (SP) tasks, and 3) complex synchronization and calibration across all antennas to fully exploit the channel reciprocity for joint processing in time-division duplex (TDD) systems. These challenges present the main bottlenecks in the practical implementation of ELAA systems. We will elaborate on these challenges in detail in the next section. Addressing these challenges is central to the discussions in this paper and will be comprehensively presented in the subsequent sections, outlining both current advancements and promising future research directions to facilitate the practical deployment of ELAA systems.

In addition to the challenges discussed above, ELAA systems face an additional challenge since they naturally operate in the radiating near-field region due to the extremely large number of antennas. Unlike in the far-field, the wireless channel in the near-field region exhibits two distinct phenomena: 1) *spherical signal wavefronts*, where both the distance and the angle between the source and each antenna array element differ [46]; 2) *spatial nonstationarity*, where different parts of the antenna array may observe the same channel paths with varying power or even entirely different channel paths [2], [45], [51]. These near-field phenomena require a different treatment compared to classical wireless communication models that assume far-field plane wave propagation. Moreover,

the large physical size of ELAA systems and their operation in the near-field make them more susceptible to interference and in-site pattern distortions caused by nearby scatterers. Despite posing challenges to SP algorithm design, the near-field phenomena also offer several benefits, such as increased spatial degrees-of-freedom and an improved ability to enhance the signal strength of target receivers in wireless communications. Interested readers may refer to [47], [48], [52] for recent surveys on the near-field systems. To be complementary to [47], [48], [52], in this paper we primarily focus on the challenges of interconnection cost, computational complexity, as well as synchronization and calibration.

### D. Contributions and Organization of the Paper

There exist several overview articles about large-scale antenna systems that provide comprehensive insights into various aspects of these systems. For instance, [3], [30] offered fundamental overviews of the advantages and research challenges associated with massive MIMO systems, discussing aspects such as spatial multiplexing, energy efficiency, and hardware implementation challenges. The papers [53], [54] focused on another important enabling technique for ELAA, namely cell-free MIMO systems, and highlighted the benefits of cell-free MIMO systems in providing uniform service quality and mitigating inter-AP interference. Recent works [55], [56] focused on large-scale intelligent surfaces, such as intelligent reflecting surfaces (IRSs) and reconfigurable intelligent surfaces (RISs). More recently, near-field phenomena for ELAA systems were covered in [47], [48], [52]. Despite the invaluable contributions provided by these studies, none of them specifically focused on the distributed SP algorithm designs for ELAA systems, which are crucial for overcoming bottlenecks such as excessive interconnection costs and high computational complexity.

The goal of this paper is to provide a comprehensive survey of distributed SP algorithms tailored for three representative forms of ELAA systems. Specifically, we focus on distributed SP algorithm designs to address the challenges of interconnection cost and computational complexity encountered in ELAA systems. This emphasis ensures that this paper stands apart from existing works [3], [30], [53]–[56], while being complementary to [47], [48], [52], as none of them specifically focus on the distributed SP algorithm designs for ELAA systems. The detailed structure of the rest of this paper is as follows.

- Section II introduces the three representative forms of ELAA systems and outlines the research challenges associated with them. It clarifies that efficient distributed SP algorithms, based on the decentralized baseband processing architecture of ELAA systems, are essential for overcoming these challenges.
- Section III reviews the distributed SP algorithms for single-BS ELAA systems using DBP architectures. We first introduce the system model and signal model, then review the distributed channel estimation, distributed uplink equalization, and distributed downlink precoding algorithms. Finally, we discuss the potential errors in channel state information (CSI) and their impact on system performance.

- Section IV provides an overview of distributed SP algorithms for coordinated distributed antenna systems, with a focus on the coordinated multi-cell transmission and CF-mMIMO scenarios.
- Section V explores the interactions between emerging technologies and ELAA systems. In particular, we consider four key technologies: network-controlled repeaters, backscatter communication, RIS, and integrated sensing and communication (ISAC).
- Section VI outlines several future research directions, including distributed SP algorithms for ELAA systems in the near-field, ELAA with flexible antennas, ELAA for physical layer security, low-resolution designs for ELAA systems, and ELAA for satellite communications.
- Section VII concludes the paper.

**Notation:** Column vectors and matrices are denoted by boldfaced lowercase and uppercase letters, e.g.,  $\mathbf{x}$  and  $\mathbf{X}$ .  $\mathbb{C}^{n \times n}$  stands for the sets of  $n$ -dimensional complex matrices. The superscripts  $(\cdot)^\top$  and  $(\cdot)^H$  describe the transpose and Hermitian operations, respectively.  $\text{Tr}(\mathbf{X})$  represents the trace of  $\mathbf{X}$ .  $\|\mathbf{x}\|^2$  and  $\|\mathbf{X}\|^2$  denote squares of the Euclidean norm and Frobenius norm of vector  $\mathbf{x}$  and matrix  $\mathbf{X}$ , respectively.  $\mathcal{R}(\mathbf{X})$  returns the real part of a complex-valued matrix  $\mathbf{X}$ .  $\mathbb{E}\{\cdot\}$  represents the statistical expectation operation.  $\odot$  denotes the Hadamard (element-wise) product.

## II. ELAA IN FOCUS: REPRESENTATIVE FORMS AND RESEARCH CHALLENGES

In this section, we provide a comprehensive introduction to ELAA systems. We begin by introducing three typical forms of ELAA systems. We then discuss the significant challenges associated with these systems, primarily stemming from the use of an extremely large number of antennas. Lastly, we introduce the DBP architecture, which is acknowledged as a promising approach to overcoming these challenges.

### A. Three Forms of ELAA Systems

As shown in Fig. 1, the ELAA systems can appear in the following three forms:

- 1) **Single-BS ELAA system:** To enhance wireless communication system performance, a natural evolution of contemporary massive MIMO technology involves substantially increasing the number of antennas at the BS. Typically, this increase is by an order of magnitude, ranging from several hundreds to thousands of antennas, resulting in the ELAA system [2], [29], [30], [46]–[48]. Thanks to the unprecedented improvement in spatial resolution brought about by the extremely large number of antennas, the ELAA system is regarded as a key enabling technology for 6G, meeting several stringent key performance indicators such as spectral efficiency, energy efficiency, reliability, as well as positioning and sensing accuracy.
- 2) **Coordinated distributed antenna systems:** Instead of directly increasing the number of antennas at a BS, another approach to implementing ELAA systems is to coordinate a large network of distributed antennas for joint

transmission. Two prominent examples of such systems are the coordinated multi-cell (joint) transmission system [57], [58] and the CF-mMIMO system [44]. In particular, the coordinated multi-cell transmission system involves a central server that communicates with multiple BSs via backhaul links to facilitate coordinated transmission, which has evolved into what is known as multi-radio multi-connectivity in the 5G New Radio standard [59]. Meanwhile, in the CF-mMIMO system, multiple APs are orchestrated by a CPU through fronthaul links to jointly serve multiple users efficiently.

- 3) **ELAA system integrated with emerging technologies:** Recently, a variety of emerging communication technologies have been integrated into large-scale antenna systems to enhance performance and introduce new functionalities while maintaining manageable complexity. As illustrated in Fig. 1, we are particularly interested in four technologies: network-controlled repeaters, backscatter communication techniques, RIS, and ISAC techniques.

### B. Challenges of ELAA Systems

To fully exploit the spatial degrees of freedom offered by ELAA systems, most existing transceiver signal processing (SP) algorithms are designed for centralized implementation, relying on a centralized baseband processing (CBP) architecture, particularly in the single-BS scenario. Such CBP architecture has been widely used in recent multi-user massive MIMO testbed implementations, such as the Argos testbed [60], [61], the LuMaMi testbed [62], [63], and the BigStation testbed [64]. In the CBP architecture, signals from all antennas are pooled and processed in a centralized baseband processor, e.g., the cloud server or the CPU. However, as the number of antennas grows, these centralized algorithms begin to face the following challenges:

- **Excessive interconnection cost:** The rapid growth in the number of BS antennas generates a substantial amount of raw baseband data, including CSI, transmit and received signals, which need to be exchanged between the CBP unit and distributed units. This results in a high communication burden and network delays when the interconnection bandwidth is limited. As an example, Fig. 2(a) illustrates the fronthaul costs of the centralized channel estimation and uplink equalization versus number of antennas. The fronthaul cost is measured by the number of complex numbers sent from the antennas to the central processor. As shown, the fronthaul cost increases linearly with the number of BS antennas. Another analysis conducted by the work [65] show that the raw baseband data throughput exceeds 1 Tbps for a massive MIMO BS operating at 80 MHz bandwidth with 256 BS antennas and 12-bit digital-to-analog converters. Such demanding bandwidth requirement severely exceeds current BS internal interface standards such as the enhanced common public radio interface [66].
- **High computational complexity:** The large number of antennas also results in high-dimensional signal processing problems. For example, the conventional linear

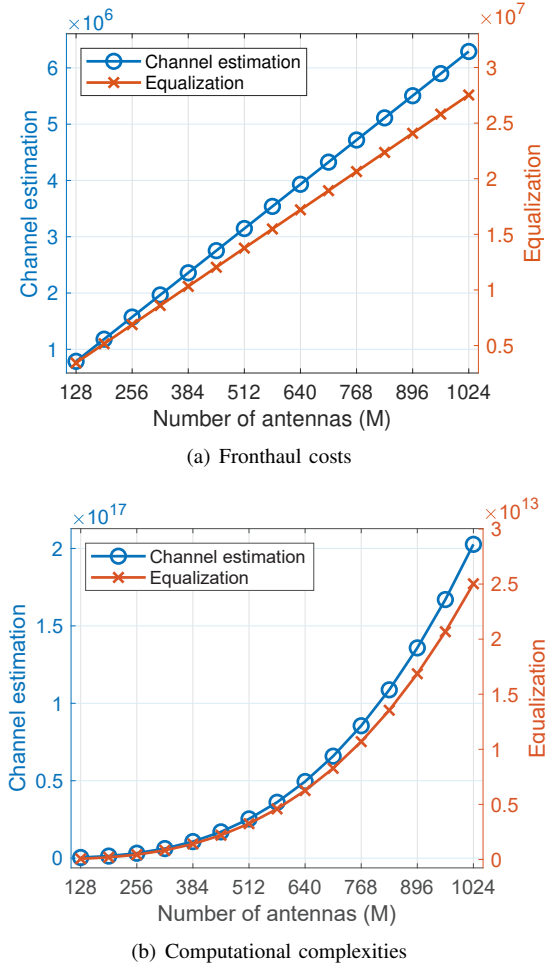


Fig. 2: The fronthaul costs (Fig. 2(a)) and computational complexities (Fig. 2(b)) of the centralized channel estimation algorithm and equalization algorithm based on the LMMSE criteria, where we use a setting of 192 subcarriers (i.e., 16 resource blocks), 32 users, and 140 symbols.

minimum mean square error (LMMSE) estimator, commonly employed for channel estimation and equalization, requires high-dimensional matrix inversion operations. The computational complexity of these operations scales cubically with the number of BS antennas in practical scenarios with cross-cell interference, making it increasingly impractical for ELAA systems where the complexity becomes prohibitively expensive. This challenge is illustrated in Fig. 2(b), which simulates the computational complexities of centralized channel estimation and uplink equalization with different number of antennas based on the LMMSE criterion.

- **Complex synchronization and calibration:** Relying on channel reciprocity in time division duplex (TDD) systems offers an efficient way to simplify downlink channel estimation in ELAA systems. However, due to the inherent non-reciprocity of transceiver hardware, synchronization and calibration are essential to effectively exploit channel reciprocity in practice. Owing to the extremely large number of antennas, achieving high-

precision synchronization and calibration can be even more challenging.

The combination of these challenges represents a major bottleneck in ELAA systems, not only degrading system efficiency but also imposing significant limitations on scalability.

### C. ELAA with Decentralized Baseband Processing

It is noted that in the coordinated distributed antenna systems and the ELAA system integrated with emerging technologies, each BS/AP is equipped with a local baseband unit (BBU) which can be exploited for processing locally received signals. This means that, although many of the existing algorithms are designed for centralized implementation in these systems, they also inherently possess a DBP architecture. Compared to CBP architecture, the DBP architecture has the following advantages. First, a DBP architecture allows the distributed nodes (DNs) to exchange some locally processed (low-dimensional) intermediate results, thereby reducing the interconnection costs. Second, since each DN only needs to process a low-dimensional received signal, the computational complexity in each DN can be significantly reduced. Last but not least, the DBP architecture improves the scalability and robustness of ELAA systems, as adding or removing a BS/AP simply amounts to adding or removing a computing unit. Therefore, one can leverage the DBP architecture to overcome the bottlenecks of excessive interconnection cost and high computational complexity by developing efficient distributed/decentralized SP algorithms.

Recently, the DBP architecture has also been introduced to the single-BS ELAA system [65]. As depicted in Fig. 3, the antennas are grouped into several non-overlapping clusters, with each cluster equipped with an independent and cost-effective BBU. Each antenna cluster, in conjunction with its local BBU, forms a DN which functions analogously to a BS or an AP in distributed antenna systems. These DNs are interconnected using various network topologies, such as the star topology and the daisy-chain topology, through fronthaul links. This architecture enables DNs to communicate and coordinate for joint transmission, while simultaneously maintaining low complexity through the use of efficient distributed SP algorithms.

Although the DBP architecture presents a promising solution to challenges such as excessive interconnection costs and high computational complexity faced by conventional CBP architectures, its effectiveness relies heavily on the development of efficient distributed SP algorithms. In the following sections, we provide a comprehensive overview of distributed SP algorithms for ELAA systems, specifically designed to address these critical bottlenecks.

## III. DISTRIBUTED SP FOR SINGLE-BS ELAA SYSTEMS

In this section, we delve into the intricacies of distributed SP algorithms tailored for single-BS ELAA systems employing the DBP architecture. We begin by introducing the system model of ELAA with DBP, laying the foundation for understanding the distributed SP framework. Next, we provide a comprehensive overview of key signal processing



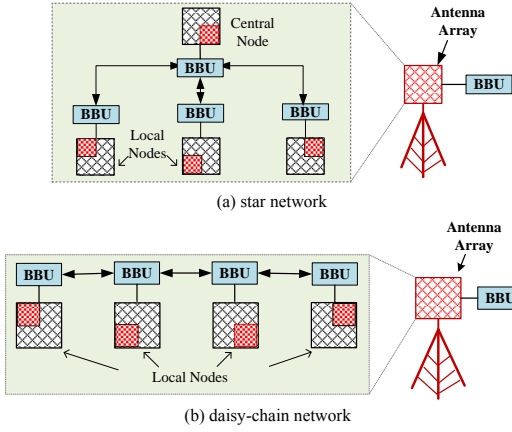


Fig. 3: Single-BS ELAA system with antenna clustering-based DBP architecture.

tasks, encompassing channel estimation, uplink equalization, and downlink precoding, which are crucial for optimizing performance in ELAA systems. Finally, we focus on the synchronization and calibration algorithms, pivotal for achieving coherent distributed processing in ELAA systems.

#### A. System Model

Consider a multi-carrier ELAA system where a single BS equipped with  $M$  antennas serves  $L$  single-antenna users over  $N_{sc}$  subcarriers. We assume that the antennas within a single panel are spaced at half-wavelength ( $\lambda/2$ ) apart, which is a typical setting in contemporary massive MIMO systems. The antennas of the BS are divided into  $C$  non-overlapping antenna clusters, with each cluster consisting of  $M_i$  antennas, where  $\sum_{i=1}^C M_i = M$ , and connecting to an independent BBU to handle its received signal. For ease of notation, we refer to an antenna cluster together with its BBU as a DN. Each performs local signal processing, including channel estimation, uplink equalization, and downlink precoding. The DNs are coordinated to improve the system performance. According to the way of information exchange, the DNs connect as different distributed architectures, e.g., the star network or the daisy-chain network, as shown in Fig. 3. Based on this model, we overview the DSP algorithm designs for ELAA using DBP architecture in the following subsections.

#### B. Channel Estimation

Consider an orthogonal case and focus on the channel estimation of one user. The antenna-and-frequency domain received pilot signal at DN  $i$  is given by

$$\mathbf{Y}_i = \mathbf{H}_i \mathbf{P} + \mathbf{N}_i \in \mathbb{C}^{M_i \times N_{sc}}, i \in \mathcal{C} \triangleq \{1, \dots, C\}, \quad (1)$$

where  $\mathbf{H}_i \in \mathbb{C}^{M_i \times N_{sc}}$  is the antenna-and-frequency domain channel between the user and DN  $i$ ,  $\mathbf{N}_i \in \mathbb{C}^{M_i \times N_{sc}}$  is the received noise at DN  $i$ ,  $\mathbf{P} \in \mathbb{C}^{N_{sc} \times N_{sc}}$  denotes the pilot matrix. The idea of distributed channel estimation (DCE) is that each DN exploits the local received signal  $\mathbf{Y}_i$  and coordinates with the other DNs to approach the performance of the centralized CE algorithm.

There are only a few works in the literature that have studied the DCE problem [67]–[71]. Specifically, [67] assumes that the antennas are deployed in a uniform planar array, with each antenna equipped with a BBU that can communicate only with its neighbors. Under this setting, an iterative DCE algorithm was proposed. However, this algorithm does not exploit channel sparsity in the angle and delay domains. To improve estimation accuracy, angle-domain channel sparsity was exploited in [68], [69], where two distributed algorithms based on an accelerated projection-based consensus method and the orthogonal matching pursuit method were proposed, respectively, to address the sparse channel estimation problem. Nonetheless, all the proposed DCE algorithms in [67]–[69] are iterative in nature, which leads to significant processing delays due to frequent information exchanges among the DNs. Additionally, the computational complexity linearly increases with the number of iterations. Furthermore, channel sparsity in the delay domain was not fully exploited in these works, thus suffering a further performance loss. Recently, to overcome these disadvantages, [71] proposed a low-complexity sparse aggregation-based DCE framework, which can perform as well as centralized schemes while maintaining low fronthaul costs and a computational complexities. In the next subsection, we will elaborate on this DCE framework in detail.

1) *Sparse Aggregation-Based DCE Framework:* In [71], the low-complexity diagonal MMSE (DMMSE) estimator is considered, while the developed DCE framework applies to other powerful estimators, e.g., the LMMSE estimator [72], [73] and compressed sensing-based estimators [74], [75]. By concatenating the received signals, channel matrices, and noise matrices, we have  $\mathbf{Y} = [\mathbf{Y}_1^H, \mathbf{Y}_2^H, \dots, \mathbf{Y}_C^H]^H$ ,  $\mathbf{H} = [\mathbf{H}_1^H, \mathbf{H}_2^H, \dots, \mathbf{H}_C^H]^H$ , and  $\mathbf{N} = [\mathbf{N}_1^H, \mathbf{N}_2^H, \dots, \mathbf{N}_C^H]^H$ . Here, for simplicity, we assume that the pilot matrix is an identical matrix. Then, based on the DMMSE estimator [76], the centralized channel estimation is to solve

$$\min_{\mathcal{S}} \mathbb{E} \{ \|\mathcal{S} \odot \mathbf{Y} - \mathbf{H}\|_F^2 \}, \quad (2)$$

where  $\mathbf{Y} = \mathbf{F}_M^H \mathbf{Y} \mathbf{F}_{N_{sc}}^H$  and  $\mathbf{H} = \mathbf{F}_M^H \mathbf{H} \mathbf{F}_{N_{sc}}^H$  are the angle-and-delay domain received signal and channel matrix, respectively, with  $\mathbf{F}_M \in \mathbb{C}^{M \times M}$  and  $\mathbf{F}_{N_{sc}} \in \mathbb{C}^{N_{sc} \times N_{sc}}$  denoting the associated discrete Fourier transformation (DFT) matrices;  $\mathcal{S} \in \mathbb{C}^{M \times N_{sc}}$  is the DMMSE estimator, and ‘ $\odot$ ’ signifies the Hadamard (element-wise) product operator. It is noted that problem (2) focuses on the angle-and-delay domain channel estimation for two primary reasons. Firstly, unlike the LMMSE estimator which is equivalent when being applied in the angle-and-delay domain and in the antenna-and-frequency domain, the DMMSE estimator is preferable in the angle-and-delay domain since it can achieve a lower mean square error (MSE) performance [71, Theorem 1]. Secondly, as will be demonstrated, estimating the channel from the angle and delay domains is essential for reducing both fronthaul costs and computational complexity in the DCE algorithm.

The DMMSE estimator in problem (2) actually performs entry-wise channel estimation, and the  $(m, j)$ -th entry of the DMMSE estimator  $\mathcal{S}$  is given by  $[\mathcal{S}]_{m,j} = \frac{[\mathbf{R}_{\mathcal{H}}]_{m,j}}{[\mathbf{R}_{\mathcal{H}}]_{m,j} + \sigma_w^2}$ ,  $m \in \mathcal{M} \triangleq \{1, \dots, M\}$ ,  $j \in \mathcal{N}_{sc} \triangleq \{1, \dots, N_{sc}\}$ . Here,  $\mathbf{R}_{\mathcal{H}} \triangleq$

$\mathbb{E}\{\mathbf{H} \odot \mathbf{H}^*\} \in \mathbb{R}^{M \times N_{sc}}$  is the power profile of  $\mathbf{H}$ . Then, the centralized angle-and-delay domain channel estimate can be written as

$$\hat{\mathbf{H}} = \mathcal{S} \odot \left( \sum_{i=1}^C \mathbf{F}_i^H \mathbf{Y}_i \mathbf{F}_{N_{sc}}^H \right), \quad (3)$$

where  $\mathbf{F}_i \in \mathbb{C}^{M \times M_i}$ ,  $i \in \mathcal{C}$ , is the  $i$ -th submatrix of  $\mathbf{F}_M$  by partitioning it horizontally into  $C$  submatrices, i.e.,  $\mathbf{F}_M = [\mathbf{F}_1^H, \mathbf{F}_2^H, \dots, \mathbf{F}_C^H]^H$ .

Given the decomposable structure in (3) over DNs and exploiting the angle-and-delay domain sparsity of the wireless channel, [71] proposed a low-complexity DCE framework based on two different strategies – first aggregating information from DNs followed by estimating the channel, or first estimating the channels at DNs followed by aggregating the estimates. These two strategies lead to two low-complexity DCE algorithms, namely, the aggregate-then-estimate (AGE) based and estimate-then-aggregate (EAG) based algorithms. In what follows, we give a brief introduction to the AGE-based algorithm in the star-networked topology shown in Fig. 3(a). Specifically, the AGE-based algorithm consists of the following three steps:

**i) Processing at DNs:** Each DN first performs an inverse discrete Fourier transform (IDFT) operation to transform the local received antenna-and-frequency domain signals into sparse antenna-and-delay domain signals. Then, each DN performs a local windowing operation on the local antenna-and-delay domain signals to divide them into two parts. The part with larger values will be sent to the CN for centralized channel estimation, while the part with smaller values will be used for local channel estimation at each DN.

**ii) Processing at CN:** After receiving the sparse antenna-and-delay domain signals from the DNs, the CU performs an IDFT operation on each antenna-and-delay domain signal with the corresponding  $\mathbf{F}_i$  in (3) to transform them into the angle-and-delay domain. Then, the angle-and-delay domain signals of all DNs are aggregated by summing them together. The centralized channel estimation is performed on the aggregated angle-and-delay domain signal. After that, the CN performs a DFT operation on the centralized estimate to transform it into antenna-and-delay domain channel estimates and sends them to the corresponding DNs.

**iii) Post-processing at DNs:** Each DN combines the centralized channel estimate and the local channel estimate to obtain the complete local antenna-and-delay domain channel estimate. Finally, the antenna-and-frequency domain channel estimate of each DN is obtained by performing a DFT operation on the local antenna-and-delay domain channel estimate.

The AGE-based algorithm can also be directly applied to the daisy-chain network. The only difference is how the signals are exchanged among nodes. The detailed signal exchange processes of AGE-based algorithm in the two networks are given in Fig. 4.

The proposed EAG-based algorithm in [71] performs similar to the AGE-based algorithm. Specifically, by the EAG-based algorithm, each DN first estimates its local CSI in the angle-and-delay domain and then sends them to the CN

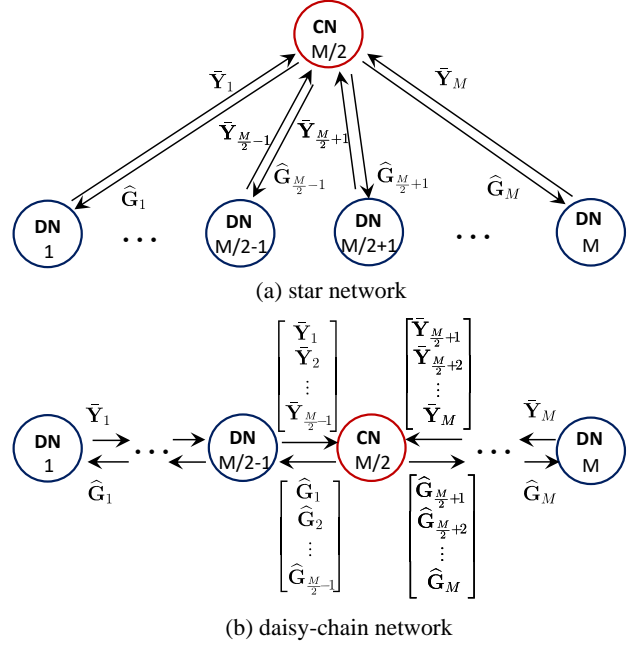


Fig. 4: Illustration of the signal exchange processes of the AGE-based algorithm in (a) the star network and (b) the daisy-chain network.

for aggregation and refined estimation. Since both the angle-and-delay domain sparsities are exploited, the EAG-based algorithm can achieve a similar performance as the AGE-based algorithm but with an even smaller fronthaul cost. As a tradeoff, the computational complexity of the EAG-based algorithm is slightly higher than the AGE-based algorithm due to the refined estimation at the CN.

Compared to the DCE algorithms in [67]–[69], the primary merits of the AGE- and EAG-based algorithms are that they only require one roundtrip exchange information between BBUs. As a result, the computational complexity and fronthaul cost are significantly reduced. In addition, AGE- and EAG-based algorithms exploit the channel sparsity in the angle and delay domains and allow flexible control of the tradeoff between fronthaul cost and estimation accuracy. Numerical results in [71] show that the overall computational complexities of both algorithms are far smaller than that of the centralized scheme, and the computation loads are evenly distributed among all BBUs. This implies that these DCE algorithms are scalable with an increasing number of DNs. Besides, the proposed algorithms can achieve a comparable MSE performance as the centralized scheme with significantly reduced fronthaul costs in both low and high signal-to-noise ratio (SNR) regimes.

**2) Future Work:** One crucial direction for future research in channel estimation for ELAA systems involves addressing the pilot contamination problem. The existing DCE algorithms have assumed that different users are scheduled on different pilot signals to avoid interference. However, the future of wireless communication aims to support a significantly larger number of users, while the number of available pilot signals remains limited. This limitation results in the pilot contamination problem, where the reuse of pilot signals among different

users introduces interference and significantly reduces channel estimation accuracy. Thus, developing DCE algorithms capable of effectively mitigating pilot contamination is crucial for enhancing the performance of ELAA systems.

### C. Uplink Equalization

Advanced multiuser equalization (MUE) techniques capable of leveraging the gain offered by the massive antennas play an important role in SP algorithm designs for ELAA systems. For uplink equalization, the received signal at DN  $i$  on subcarrier  $j$  is given by

$$\mathbf{y}_{i,j} = \mathbf{H}_{i,j}\mathbf{s}_j + \mathbf{u}_{i,j}, i \in \mathcal{C}, j \in \mathcal{N}_{sc}, \quad (4)$$

where  $\mathbf{H}_{i,j} \in \mathbb{C}^{M_i \times L}$  is the channel between DN  $i$  and the  $L$  users,  $\mathbf{s}_j \in \mathbb{C}^{L \times 1}$  denotes the users' signal, and  $\mathbf{u}_j \in \mathbb{C}^{M_i \times 1}$  is the (colored or white) noise. In the literature, the LMMSE-based equalizer is widely used owing to its low computational complexity compared to the nonlinear maximum-likelihood detector and its high performance compared to the linear counterparts, such as the maximum ratio combining (MRC) and zero-forcing (ZF) based detectors [30]. By letting  $\mathbf{y}_j = [\mathbf{y}_{1,j}^\top, \mathbf{y}_{2,j}^\top, \dots, \mathbf{y}_{C,j}^\top]^\top$  and based on the LMMSE criteria, the centralized equalization problem can be formulated as

$$\min_{\mathbf{W}_j} \mathbb{E} [\|\mathbf{s}_j - \mathbf{W}_j \mathbf{y}_j\|^2], \forall j \in \mathcal{N}, \quad (5)$$

where  $\mathbf{W}_j = [\mathbf{W}_{1,j}, \mathbf{W}_{2,j}, \dots, \mathbf{W}_{C,j}]$  is the equalizer with  $\mathbf{W}_{i,j} \in \mathbb{C}^{L \times M_i}$  representing the equalizer for DN  $i$ .

Based on the decomposable structure of (5) over DNs, several works have studied the distributed/decentralized equalization algorithm designs in the literature [77]–[86]. In particular, considering a star or a daisy-chain network, the works [77]–[81] investigated the uplink MUE problem based on the iterative approximate message passing algorithm, while the MRC and LMMSE-based MUE methods are studied in [82]. Recently, considering an extremely large-scale MIMO system, [83] studied the decentralized MUE problem under the spatially non-stationary channel model. While most existing works considered the star or daisy-chain topologies, [84] investigated the decentralized equalization in a ring topology under the DBP architecture. Despite these promising improvements, the previous works all have assumed that the additive noise is spatially white while ignoring the inter-cell interference. Besides, these algorithms require iterative information exchanges between distributed nodes, which could incur a large amount of fronthaul cost. Therefore, these algorithms may not be applicable to the practical systems where the inter-cell interference exists and the fronthaul bandwidth is limited.

On the other hand, the number of antennas in each DN could be much larger than the number of users in massive MIMO systems, indicating that the received signal at each DN contains considerable redundancy. This observation motivates compression-based equalization schemes under the DBP architecture, where the DNs first compress the local received signal to remove the redundancy and then forward the (low-dimensional) compressed signal to the CN for joint equalization. This compression-and-forward strategy has been widely studied for bandwidth-limited systems, for example,

the fronthaul/backhaul capacity-limited cloud radio access network (C-RAN) [87]–[92], where the compression is implemented by using sophisticated source coding methods, e.g., the Wyner-Ziv coding in [87], [88], [91]. As an important branch of compression schemes, linear compression (LC) has been investigated in sensor networks for distributed parameter compression-estimation, in view of its low complexity [93]–[96]. In particular, in such systems, the distributed sensors first linearly compress their local received signals and then send them to a fusion center for joint estimation. Considering the advantages of the LC scheme in reducing fronthaul costs and its low computational complexity, the LC-based approach is seen as a promising solution to address the limitations of fronthaul bandwidth and the computational capabilities of baseband units (BBUs) in practical ELAA systems. In light of this, the LC-based MUE (LC-MUE) schemes have been proposed in [97], [98]. In what follows, we give an introduction to the LC-MUE schemes in the literature, primarily focusing on the practical multi-carrier case [98].

1) *LC-MUE Scheme for Multi-Carrier Systems*: The idea of the LC-MUE scheme is analogous to the LC-based distributed parameter compression-estimation in [93]–[96], which is implemented through the following steps:

- i) The CN jointly designs the compressors and the equalizers for each subcarrier by solving the JCDE problem;
- ii) The CN sends the compressors to the DNs for compressing the received signals;
- iii) The DNs send the locally compressed signals to the CN for centralized equalization using the equalizers designed in step i).

An illustration of the information exchange process of the LC-MUE scheme is depicted in Fig. 5. It is noted that, since the number of compressors is proportional to the number of subcarriers, the compressor may be shared across multiple subcarriers to save the fronthaul cost.

As shown in Fig. 5, the fronthaul cost of the LC-MUE scheme consists of two parts. One is for delivering optimized compressors from the CN to DNs, and the other is for sending the compressed signals from DNs to the CN. So, the total fronthaul cost of the LC-MUE scheme is  $\sum_{i=1}^C M_i r_i + N_{sc} N_{sym} \sum_{i=1}^C r_i$  where  $N_{sym}$  denotes the number of symbols that the channel keeps invariant. Therefore, compared to the traditional LMMSE scheme, which has a fronthaul cost of  $M N_{sc} N_{sym}$ , the overall fronthaul cost of the LC-MUE scheme is expected to be reduced substantially when  $r_i$ 's are small, and when  $M$  and  $N_{sc}$  are large. For example, for the case with  $M = 256$ ,  $N_{sc} = 128$ ,  $N_{sym} = 14$ ,  $L = 32$ ,  $r_i = 16, \forall i$ , and  $C = 4$ , the fronthaul cost of the LC-MUE scheme is only 25.9% of the conventional centralized LMMSE scheme.

Based on the above model and the LMMSE criteria, the LC-MUE scheme involves solving a multi-carrier joint compression and data equalization (MC-JCDE) design problem to minimize the equalization MSE, which is given by

$$\min_{\substack{\{\mathbf{U}_j\}_{j=1}^{N_{sc}}, \\ \mathbf{V} \text{ block diagonal}}} \sum_{j=1}^{N_{sc}} \mathbb{E} [\|\mathbf{s}_j - \mathbf{U}_j \mathbf{V} \mathbf{y}_j\|^2], \quad (6)$$



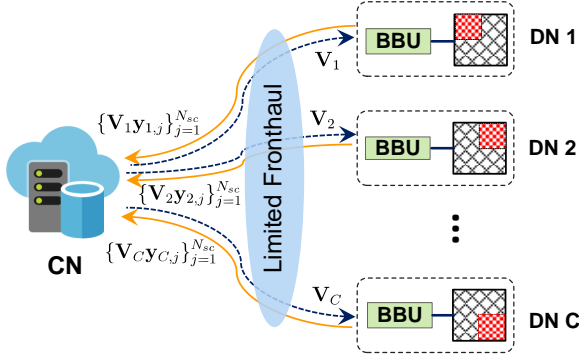


Fig. 5: Illustrations of the DBP architecture.

where  $U_j \in \mathbb{C}^{L \times r}$  is the LMMSE equalizer for each subcarrier  $j$ , and  $\mathbf{V} = \text{blkdiag}(\mathbf{V}_1, \dots, \mathbf{V}_C) \in \mathbb{C}^{r \times M}$  is the compressor, which is block-diagonal with  $\mathbf{V}_i$  on the  $i$ -th diagonal block,  $r = \sum_{i=1}^C r_i$  with  $r_i < M_i$  denoting the compressed dimension of DN  $i$ . It is worthy to note that when the flat-fading channel, e.g.,  $N_{sc} = 1$ , is considered, problem (6) reduces to the problem studied in [93]–[97], which can be efficiently solved by the block coordinate descent (BCD) algorithm. However, the BCD algorithm is no longer efficient for (6), since updating the compressor  $\{\mathbf{V}_i\}$  involves computing a matrix inversion of dimension  $M_i r_i \times M_i r_i$ . To address this issue, several low-complexity algorithms have been proposed in [98]. In the following, we briefly discuss these algorithms.

**(1) BCD-ADMM Algorithm:** Rather than solving problem (6) directly, the BCD-ADMM algorithm considers the following problem to update compressor  $\mathbf{V}_i$ :

$$\min_{\mathbf{V}_{i,a}, \mathbf{V}_{i,b}} \sum_{j=1}^{N_{sc}} \text{Tr} \left( U_{i,j}^k \mathbf{V}_{i,a} \mathbf{R}_{\mathbf{y}_{i,j}} \mathbf{V}_{i,b}^H (U_{i,j}^k)^H - \mathcal{R}(U_{i,j}^k (\mathbf{V}_{i,a} + \mathbf{V}_{i,b}) \mathbf{R}_{\mathbf{y}_{i,j}}^k) \right) \quad (7a)$$

$$\text{s.t. } \mathbf{V}_{i,a} = \mathbf{V}_{i,b}. \quad (7b)$$

Problem (7) can be solved by the nonconvex ADMM method [99], [100]. Interestingly, as shown by [98, Theorem 1], the ADMM algorithm can actually converge to same  $\mathbf{V}_i$  as the BCD algorithm. Another merit of the BCD-ADMM algorithm is that it only involves low-dimensional matrix multiplications (i.e.,  $M_i \times M_i$  and  $M_i \times r_i$ ), thereby having a much lower computational complexity compared to the BCD algorithm, especially when the numbers of antennas and subcarriers are large.

**(2) SVD-AGG Algorithm:** The SVD-AGG algorithm consists of three steps:

- i) A small number of subcarriers are uniformly selected from the  $N_{sc}$  subcarriers, and for each subcarrier, one solves the corresponding single-carrier JCDE problem to obtain a compressor;
- ii) For each DN  $i$ , the obtained compressors for the selected subcarriers are aggregated by a singular value decomposition (SVD)-based scheme to produce an approximated compressor, which will be shared by all subcarriers;
- iii) With the approximated compressor, the equalizer for each subcarrier is obtained accordingly.

Note that the SVD-AGG algorithm first adopts the simple carrier-wise JCDE solution, followed by a succinct aggregation step to generate a high-quality shared compressor. Therefore, it enjoys further reduced complexity compared to the BCD-ADMM algorithm.

**(3) Fully Decentralized Scheme:** The above algorithms requires the global CSI to be available at the CN, which may cause large delay by sending the local pilot signals from DNs to the CN. The fully decentralized (FD) scheme allows the DNs relies on the local information to design a local compressor by using the previous algorithms, e.g., the BCD-ADMM algorithm. Then, the equalizer for each subcarrier is obtained accordingly by assuming a block-diagonal  $\mathbf{R}_{\mathbf{y}_j}$ . Such an FD scheme can be found useful to initialize the previous algorithms for further computational complexity reductions.

**(4) Partially Decentralized Scheme:** The partially decentralized (PD) scheme can realize more flexible tradeoff between the equalization accuracy and computational complexity. Specifically, in the PD scheme, each DN first designs a local compressor relying its local information, and sends the compressed pilot signals, together with data signals, to the DU. Then, the CN utilizes the compressed pilot signal to estimate the “effective”  $\mathbf{R}_{\mathbf{y}_j}$ . Finally, the equalizer for each subcarrier is obtained by using the estimated  $\mathbf{R}_{\mathbf{y}_j}$  and the received compressed signals. It is noted that, if the local compressed dimension is set to the number of users and the flat-fading channel is considered, the PD scheme reduces to the “cDR-MMSE” scheme in [97].

**2) Future Work:** In practical TDD systems, uplink interference is estimated using the demodulation reference signal (DMRS), which is transmitted alongside the uplink user data. Previous schemes assume that full interference information is available at the CN, implying that the DNs must send the DMRSs to the CN for centralized interference estimation. Given that the DMRS and uplink user data are transmitted together, sending the DMRSs to the CN could incur a high processing delay, making it unsuitable for applications with strict delay requirements. Therefore, it is of interest to investigate efficient LC-MUE schemes that assume that the interference signal is only available at the DNs.

#### D. Downlink Precoding

Downlink precoding is a fundamental SP technique in ELAA systems to manage inter-user interference and enhance signal strength at the receiver end, thereby increasing the system spectral efficiency. Under the DBP architecture, the received signal at user  $k$  on the  $j$ -th subcarrier is given by

$$\begin{aligned} \mathbf{y}_k^{(j)} &= \mathbf{H}_k^{(j)} \mathbf{Z}_k^{(j)} \mathbf{s}_k^{(j)} + \sum_{\ell \neq k}^K \mathbf{H}_k^{(j)} \mathbf{Z}_\ell^{(j)} \mathbf{s}_\ell^{(j)} + \mathbf{n}_k^{(j)} \\ &= \sum_{i=1}^C \mathbf{H}_{i,k}^{(j)} \mathbf{Z}_{i,k}^{(j)} \mathbf{s}_k^{(j)} + \sum_{\ell \neq k}^K \sum_{i=1}^C \mathbf{H}_{i,k}^{(j)} \mathbf{Z}_{i,\ell}^{(j)} \mathbf{s}_\ell^{(j)} + \mathbf{n}_k^{(j)}, \end{aligned} \quad (8)$$

where  $\mathbf{H}_{i,k}^{(j)} \in \mathbb{C}^{N_k \times M_i}$  is the channel between the DN  $i$  and user  $k$  on subcarrier  $j$ ,  $\mathbf{Z}_{i,k}^{(j)} \in \mathbb{C}^{M_i \times L_k}$  is the corresponding precoder for user  $k$ ,  $\mathbf{s}_k^{(j)} \in \mathbb{C}^{L_k \times 1}$  represents the signal for

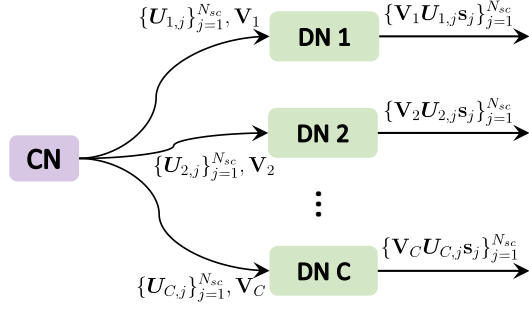


Fig. 6: Illustrations of the DBP architecture.

user  $k$ , and  $\mathbf{n}_k^{(j)} \in \mathbb{C}^{N_k \times 1}$  is the AWGN at user  $k$  with  $N_k$  denoting the number of received antenna at user  $k$ . Then, the sum-rate maximization problem can be formulated as

$$\max_{\{\mathbf{z}_{i,k}^{(j)}\}} \sum_{j=1}^{N_{sc}} \sum_{k=1}^K R_k^{(j)} \quad (9a)$$

$$\text{s.t.} \quad \sum_{j=1}^{N_{sc}} \sum_{k=1}^K \sum_{i=1}^C \text{Tr}(\mathbf{z}_{i,k}^{(j)} (\mathbf{z}_{i,k}^{(j)})^H) \leq P_{\max}, \quad (9b)$$

where  $P_{\max}$  is the maximum transmission power of the BS, and

$$R_k^{(j)} = \log \det \left\{ \mathbf{I} + \sum_{i=1}^C \mathbf{H}_{i,k}^{(j)} \mathbf{z}_{i,k}^{(j)} (\mathbf{H}_{i,k}^{(j)} \mathbf{z}_{i,k}^{(j)})^H \right. \\ \left. \left[ \sum_{\ell \neq k}^K \sum_{i=1}^C \mathbf{H}_{i,\ell}^{(j)} \mathbf{z}_{i,\ell}^{(j)} (\mathbf{H}_{i,\ell}^{(j)} \mathbf{z}_{i,\ell}^{(j)})^H + (\sigma_k^{(j)})^2 \mathbf{I} \right]^{-1} \right\} \quad (10)$$

is the achievable data rate of user  $k$  on subcarrier  $j$ .

There have been numerous studies on distributed/decentralized precoding algorithm design based on a model similar to that of (9) [101]–[107]. Specifically, [65], [103] proposed several distributed precoding algorithms based on Zero-Forcing (ZF) and Wiener Filter (WF) methods, while [105] explored the trade-off between computational complexity and fronthaul cost under the DBP architecture. Recently, [107] introduced two decentralized precoding algorithms based on Eigen Zero-Forcing (EZF) and weighted minimum mean square error (WMMSE) precoding schemes, respectively, to achieve communication-efficient designs. Despite these promising advancements, existing works primarily focus on designing distributed algorithms for the DBP architecture without adequately addressing the limitations of computational complexity and fronthaul cost. Moreover, these algorithms are mainly developed for single subcarrier scenarios and are not applicable to multi-carrier systems with limited interconnection bandwidth, restricting their practical applicability.

On the other hand, it is noted that in ELAA systems, the number of antennas in each DN can be significantly larger than the number of data streams. This provides an opportunity to design a compression-based precoding scheme to reduce the interconnection cost. In the literature, compression-based methods have been studied for distributed wireless networks to reduce fronthaul costs [87]–[89], [91], [108].

For example, quantization-based compression methods were investigated in [88], [91], [108] to reduce the fronthaul cost of C-RAN with finite fronthaul capacity. As discussed in the subsection on uplink equalization, the LC-based method is efficient for reducing fronthaul costs, which motivates the LC-based precoding (LCP) scheme. The idea of the LCP scheme was first considered in [92] for a C-RAN network. Specifically, [92] addressed a joint compressor and equalizer design problem and then directly reused the uplink compressor for the downlink by exploiting the channel reciprocity of TDD systems. However, this work focused only on single-carrier systems and considered heuristics and simple ZF precoder. Moreover, directly applying the uplink compressor to the downlink could lead to performance loss, as the colored noise in the downlink generally differs from that in the uplink. To overcome these disadvantages, it is urgent to develop a more sophisticated LCP scheme for the ELAA system using DBP architecture. Recently, [98] considered the LCP scheme for a practical multi-carrier ELAA system using DBP architecture, as shown in Fig. 6.

1) *LCP Scheme for Multi-Carrier Systems:* Similar to the uplink LC-MUE scheme, the LCP scheme for the downlink system also requires only a single roundtrip of information exchange between the CN and the DNs. The detailed workflow is outlined as follows:

- i) The CN jointly designs the compressor and precoder by solving a joint compression and precoding design (JCPD) problem;
- ii) The CN sends the precoder and compressed signals to the corresponding DNs;
- iii) The DNs precoder the compressed signals with the precoder and send the precoded signal to the users.

In this scheme, the signal on each subcarrier will be designed a compressor, while the precoder may be shared by multiple subcarriers for fronthaul reduction, since the precoder should be sent to the DNs. It is noted that the key of the LCP scheme is to efficiently solve the JCPD problem, which is given by

$$\max_{\substack{\{\mathbf{U}^j\}_{j=1}^{N_{sc}}, \\ \mathbf{V} \text{ block diagonal}}} \sum_{j=1}^{N_{sc}} \sum_{k=1}^K R_k^j \quad (11a)$$

$$\text{s.t.} \quad \sum_{j=1}^{N_{sc}} \sum_{k=1}^K \sum_{i=1}^C \|\mathbf{V}_i^H \mathbf{U}_{i,k}^{(j)}\|_2^2 \leq P_{\max}, \quad (11b)$$

where  $R_k^j$  is the achievable rate of user  $k$  on subcarrier  $j$ , which is given by  $R_k^{(j)} = \log \det \left\{ \mathbf{I} + \sum_{i=1}^C \mathbf{H}_{i,k}^{(j)} \mathbf{V}_i \mathbf{U}_{i,k}^{(j)} (\mathbf{H}_{i,k}^{(j)} \mathbf{V}_i \mathbf{U}_{i,k}^{(j)})^H \left[ \sum_{\ell \neq k}^K \sum_{i=1}^C \mathbf{H}_{i,\ell}^{(j)} \mathbf{V}_i \mathbf{U}_{i,\ell}^{(j)} (\mathbf{H}_{i,\ell}^{(j)} \mathbf{V}_i \mathbf{U}_{i,\ell}^{(j)})^H + (\sigma_k^{(j)})^2 \mathbf{I} \right]^{-1} \right\}$ ,  $\mathbf{U}_{i,k}^j \in \mathbb{C}^{L \times r_i}$  is the compressor for user  $k$  on subcarrier  $j$ , and  $\mathbf{V}_i \in \mathbb{C}^{r_i \times M}$  is the shared precoder.

Compared to (9), the LCP problem (11) is much more challenging to solve owing to the coupling of the compressors and precoder in both the objective function and constraints [109]. To solve problem (11) efficiently, [110] proposed two algorithms based on a penalty dual decomposition (PDD) method and a matrix factorization (MF) method, respectively. Specifically, the PDD-based algorithm jointly optimizes the compressor and precoder, which achieves a promising per-

formance but with a high computational complexity. While the MF-based algorithm aims to solve problem (11) in a low-complexity manner. In what follows, we give a brief introduction to the MF-based algorithm

Basically, the MF-based algorithm consists of the following two steps:

- i) One solves the conventional precoding design problem in (9) to obtain a set of precoders,  $\mathbf{Z}_k^{(j)}$ , for all subcarriers. In particular, the precoders can be obtained by using the well-known WMMSE algorithm [111] or the EZF algorithm [112].
- ii) With the attained precoders, one solves the following low-rank MF problem to obtain the compressors and the shared precoder

$$\min_{\{\mathbf{V}_i, \tilde{\mathbf{U}}_i\}} \sum_{i=1}^C \|\tilde{\mathbf{Z}}_i - \mathbf{V}_i \tilde{\mathbf{U}}_i\|_F^2, \quad (12)$$

where  $\tilde{\mathbf{Z}}_i = [\mathbf{Z}_i^{(1)}, \dots, \mathbf{Z}_i^{(N_{sc})}] \in \mathbb{C}^{M_i \times LN_{sc}}$ , and  $\tilde{\mathbf{U}}_i = [\mathbf{U}_i^{(1)}, \dots, \mathbf{U}_i^{(N_{sc})}] \in \mathbb{C}^{r_i \times LN_{sc}}$ . To obtain the factorization results efficiently, the SVD operation is performed on  $\tilde{\mathbf{Z}}_i$  and utilize the first  $r_i$  columns of right singular matrix to construct  $\tilde{\mathbf{U}}_i$ . The corresponding  $\mathbf{V}_i$  is determined by the least squares solution. Finally, the  $\mathbf{U}_{i,k}^{(j)}$  are scaled to ensure that the power constraints are active.

The MF-based algorithm has comparable computational complexity to the conventional centralized precoding scheme, since the second step only performs a low-complexity MF operation, making it preferable in practical applications where powerful servers are not available.

#### E. Accuracy of the CSI, and Phase Calibration

There are four different error sources in the CSI (channel estimates) in large-scale and distributed MIMO: (a) noise and interference on the channel estimates; (b) channel aging (the fact that estimates become outdated); (c) errors resulting from uplink-downlink reciprocity imbalances within an array; and (d) errors resulting from oscillator drifts (accumulated phase noise) when different service antennas in an array, or different distributed arrays, are driven by oscillators that are not mutually phase-locked. In what follows, we discuss these different errors sources and how they can be mitigated:

- (a) **Noisy channel estimates:** Noisy channel estimates can be a significantly limiting factor, especially on uplink where the available power is generally smaller. The countermeasures are to increase power (to the extent permitted) and to increase the integration gain (length of the pilot sequences); see [33].

Interference on the channel estimates can originate either from reuse of pilots or from data transmission on the pilot dimensions in other cells; both are equally bad [33, Sec. 4.4.3]. The countermeasures are sparse enough pilot reuse [33, Chap. 6], and the use of second-order statistics of the fading process to improve the channel estimates [113] – effectively, spatially filtering the received pilots before estimating the channels.

- (b) **Channel aging:** In most analyses of massive and distributed MIMO, the channel is modeled as block-fading. While this is an excellent abstraction for capacity analysis and system optimization tasks such as power control, in reality the channel response varies continuously as function of time and frequency. On uplink, given pilots that are spread out over the time-frequency domain, one can easily interpolate both over time and frequency to obtain estimates for each time-frequency resource element (sample). The downlink [in TDD] is more difficult, as one has to rely on prediction, or on the (erroneous) presumption that the channel remains static once transmission has switched from uplink to downlink. Channel prediction is an active area of research; for some early contributions see [114].

- (c) **Uplink-downlink reciprocity imbalance:** Within an array, where all antennas are driven by the same local oscillator, there may be an imbalance between the phase lag in the receive and in the transmit branch; this imbalance nominally breaks the uplink-downlink reciprocity required for reciprocity-based multiuser MIMO beamforming in TDD to work. The countermeasure is reciprocity calibration. State-of-the-art methods rely on transmission between different antennas *within* the array, and taking bidirectional measurements from which the reciprocity imbalances can be estimated [60], [115]–[123]. This calibration can be done rather infrequently, since the uplink-downlink phase imbalances only change slowly over time (they are mainly dependent on external factors such as temperature).

- (d) **Oscillator drifts:** When different antennas in an array, or different panels (subarrays) are driven by independent local oscillators that are not locked in phase, calibration measurements are required to *jointly reciprocity-calibrating* the arrays.<sup>2</sup> This can be done by bidirectional over-the-air measurements *between the arrays* [124]–[131]. This calibration has to be re-done every time the oscillators have drifted by some amount, which in practice means very frequently unless very stable (and expensive) oscillators are used: In contrast to the reciprocity-calibration within an array [(c) above], this calibration may have to be performed on a millisecond-level timescale. An estimation-theoretic analysis of over-the-air calibration of distributed MIMO, based on a graph representation of the who-measures-on-whom topology, can be found in [132]. Therein it is shown, in particular – and perhaps counterintuitively – that the more antennas that are involved in the calibration the less accurate the phase estimates become, but the more accurate the beamforming becomes.

Importantly, (a)–(d) affect the downlink, but only (a)–(b) affect the uplink since on uplink, pilots and data see the same channel, so neither reciprocity nor phase alignment between antennas is required. Especially the fourth effect, (d), appears to have been the source of significant misconceptions in the literature, as discussed in [133], [134].

<sup>2</sup>Also known as phase synchronization, or phase alignment.

It should be noted in this context that synchronization in an ELAA system entails several different components: synchronization in frequency between independent panels; synchronization in time; synchronization of the sampling clocks; and synchronization (alignment) of the phase for joint coherent downlink beamforming. Among these problems, it is the phase synchronization, discussed above under item d), that is the most difficult. However, open problems remain especially on how to efficiently synchronize the sampling clocks.

Given the importance of synchronization, especially phase alignment among distributed panels, the development of robust and efficient methods should be a priority for future work. For example, when introducing phase alignment measurements into the picture, the TDD flow must be broken. Specifically, an access point that is receiving calibration signals from another access point needs to reverse its operation in the sense that uplink and downlink are swapped: during one or multiple slots it must listen when other access points transmit and vice versa. This creates a host of new problems. One is that an access point that switches from transmission to reception during (a part of) a slot nominally assigned to downlink transmission will miss the opportunity to transmit on downlink to users during that part of the slot. This will affect the quality of service of the traffic, especially for low-latency applications and for cases when the access point in question is critical to or the *only one* of the access points serving a particular user. An optimization framework could be devised to determine which access points should transmit calibration signals and which access points should receive calibration signals in a given slot, taking into account the requirements of the users being served at a given point in time, the traffic situation, and the traffic's latency constraints.

#### IV. DISTRIBUTED SP FOR ELAA SYSTEMS WITH COORDINATED DISTRIBUTED ANTENNAS

In this section, we focus on the distributed SP algorithm designs for ELAA systems with coordinated distributed antennas. Specifically, we concentrate on two representative systems: the multi-cell coordinated transmission system and the CF-mMIMO system. In multi-cell coordinated transmission systems, multiple massive MIMO BSs coordinate to jointly serve multiple users in these cells. In CF-mMIMO systems, a central processing unit coordinates multiple APs to jointly serve multiple users in a spatial area. Since the CF-mMIMO system performs user-centric transmission, it can provide uniform performance across the network.

##### A. Similarities and Differences With the Single-BS ELAA Systems Using DBP Architectures

The considered ELAA systems with distributed antennas share a similar system architecture with single-BS ELAA systems using DBP architectures. Both system forms leverage the DBP architecture, allowing for distributed signal processing (SP) across multiple processing units. Consequently, many algorithms developed for single-BS ELAA systems can be applied to systems with distributed antennas. However,

there are still two key differences that necessitate further investigations.

- Firstly, in single-BS ELAA systems, it is assumed that there is always a central server (i.e., CN) capable of performing centralized processing. However, such a powerful central server may not always exist in coordinated multi-cell transmission systems, necessitating the development of more efficient distributed SP algorithm designs [135]–[137].
- Secondly, while antennas in single-BS ELAA systems are co-located, it is no longer the case in ELAA systems with distributed antennas. Under distributed antenna settings, the channels between users and some antennas may be poor due to large-scale fading. Consequently, it is not efficient to use all antennas to serve all users, particularly when considering computation- and communication-efficient distributed SP designs. Therefore, this spatial distribution introduces new research challenges, such as user association and user scheduling.

These two differences pose new research challenges, leading to distinct research problems that require innovative solutions. Addressing these challenges will be the focus of the subsequent subsections, where we will explore the developments of efficient distributed SP algorithms tailored to ELAA systems with coordinated distributed antennas.

##### B. Distributed SP for Multi-Cell Coordinated Transmission Systems

In multi-cell coordinated transmission systems, the distributed downlink precoding problem has been widely studied in the literature. However, the distributed channel estimation and uplink equalization problems have been rarely addressed. In this subsection, we primarily focus on an overview of the distributed downlink precoding algorithms and distributed user scheduling algorithms for multi-cell coordinated transmission system.

1) *Review of Existing Distributed Multi-Cell Coordinated Precoding Algorithms:* Consider a downlink multi-cell system where  $C$  BSs cooperative to serve multiple users. For ease of illustration, we assume that one user is scheduled in each cell for downlink transmission. Then, the centralized multi-cell coordinated precoding (MCP) problem in flat-fading channel is given by

$$\max_{\{\mathbf{Z}_i\}} \sum_{i=1}^C R_i \quad (13a)$$

$$\text{s.t. } \text{Tr}(\mathbf{Z}_i \mathbf{Z}_i^H) \leq P_{\max}, \forall i \in \mathcal{C}, \quad (13b)$$

where  $\mathbf{Z}_i$  is the precoder for the user in cell  $i$ , and

$$R_i = \log \det \left\{ \mathbf{I} + \mathbf{H}_{i,i} \mathbf{Z}_i (\mathbf{H}_{i,i} \mathbf{Z}_i)^H \right\} \cdot \left[ \sum_{\ell \neq i}^C \mathbf{H}_{i,\ell} \mathbf{Z}_\ell (\mathbf{H}_{i,\ell} \mathbf{Z}_\ell)^H + \sigma_i^2 \mathbf{I} \right]^{-1} \quad (14)$$

is the achievable data rate of cell  $i$ . Here,  $\mathbf{H}_{i,\ell}$  is the channel between BS  $\ell$  and the user in cell  $i$ .

The MCP problem has been widely studied in the literature [87], [111], [138]–[141], which showed that MCP is able to

eliminate both intra-cell and inter-cell interference, thereby providing considerable performance gains. However, as the number of antennas and users increases, these cooperative strategies may become less desirable due to the overheads associated with channel information exchange among BSs via backhaul links and the need for a powerful central processor. Additionally, the computational complexities of the algorithms scale rapidly with the network size. A naive approach to overcoming these challenges is to perform fully decentralized precoding, where each BS optimizes the precoders for the users in its cell solely based on local acquired CSI, while treating inter-cell interference as noise. However, in practical scenarios, the inter-cell interference is actually a bottleneck of multi-cell system, and thus the performance of fully decentralized schemes could be significantly degraded. Therefore, efficient distributed precoding algorithms, which can not only achieve promising performance but also have low inter-connection costs, are crucial for making multi-cell coordinated transmission practical.

In the literature, there have been many works studying efficient distributed MCP (D-MCP) designs [135], [142]–[147], and several promising approaches have proposed. In what follows, we give an introduction to three efficient distributed precoding approaches aiming at reducing the cost of backhaul signaling:

- **D-MCP via new metrics:** When the system cannot capture interference from other cells, it is possible to improve system performance by reducing leakage to other cells only based on local CSI. Motivated by this, the work [144] proposed a new metric, called signal-to-leakage-and-noise ratio (SLNR), which involves the amount of interference caused by desired signal on other users. Different from the conventional SINR-based schemes, the SLNR metric can decouple the optimization problem and allows fully decentralized solutions. The concept of leakage was further developed in [145] where the signal-to-leakage-plus-interference-plus-noise ratio (SLINR) is defined by simultaneously considering both the intra-cell interference and the total interference leakage to users served by other cells. The work [146] defined another expression of SLINR by changing the sum of interference leakages to the geometric mean. The associated problems can be efficiently solved by the WMMSE method. However, the discrepancy between the SLINR and the SINR may lead to performance loss in practice. Besides, the geometric-mean leakage term in [146] is expensive to compute and causes large gradient-computation overhead.
- **D-MCP via user cooperation:** Considering a TDD systems, the work [148] proposed a distributed precoding scheme with a new information exchange mechanism via user cooperation. In particular, the proposed scheme introduced a new uplink signaling resource and a new CSI combining mechanism that complement the existing uplink and downlink pilot-aided channel estimations. This enables each BS to acquire the necessary cross-term information, entirely eliminating the need for backhaul signaling for CSI exchange. However, the proposed algo-

rithm in [148] is iterative in nature, which may cause a large processing delay.

- **D-MCP via interference power exchange:** Another approach to reduce the backhaul signaling is to exchange the interference power (IFP) instead of CSI between the cooperative BSs [135], [147]. This leads to a problem that jointly optimize the precoding and IFP variables, which can be iteratively solved by the primal decomposition method [147] or the dual decomposition method [135]. During the iterations, BSs that interfere with each other only need to exchange IFP variables. However, in practical system, the IFP graph may not be the same as the backhaul graph, which brings new challenges in IFP variables exchange among BSs.

Recently, a simple yet efficient D-MCP scheme, relying on a virtual power control (VPC) based formulation, was proposed in [137]. The VPC-based formulation is similar to the centralized formulation but is solved by each BS individually based on its own CSI. Additionally, the cooperative BSs only need to exchange the interference channels to users in other cells and transmission powers. As a result, the performance can approach that of the centralized scheme but with a much reduced backhaul cost. In what follows, we give a more detailed introduction to the VPC-based D-MCP scheme.

2) *Efficient D-MCP via a VPC-based Formulation:* As seen from (13), once the interference terms, i.e.,  $\mathbf{H}_{i,\ell}\mathbf{Z}_\ell, \forall \ell \neq i$ , are given, each BS can solve the problem by itself based on local CSI. On the other hand, the interference terms can be split into two parts as  $\mathbf{H}_{i,\ell}\mathbf{Z}_\ell = \mathbf{G}_{i,\ell}\mathbf{P}_\ell$ . Here,  $\mathbf{G}_{i,\ell}$  and  $\mathbf{P}_\ell$  are respectively given by

$$\mathbf{G}_{i,\ell} = \left[ \mathbf{H}_{i,\ell} \frac{[\mathbf{Z}_\ell]_1}{\|\mathbf{Z}_\ell\|_1}, \dots, \mathbf{H}_{i,\ell} \frac{[\mathbf{Z}_\ell]_M}{\|\mathbf{Z}_\ell\|_M} \right], \quad (15a)$$

$$\mathbf{P}_\ell = \text{blkdiag}\{\|\mathbf{Z}_\ell\|_1, \dots, \|\mathbf{Z}_\ell\|_M\}, \quad (15b)$$

As seen,  $\mathbf{G}_{i,\ell}$  collects the corresponding interference channels from BS  $\ell$  to the user in cell  $i$ , and  $\mathbf{P}_\ell$  represents the transmission power to the user in cell  $\ell$ . The idea of the VPC-based scheme is to allow each BS to “virtually” control the transmission power variables of other BSs so as to predict their behaviors as if the centralized optimization is conducted. In particular, by inserting  $\mathbf{G}_{i,\ell}$  and  $\mathbf{P}_\ell$  into  $R_i$  in problem (13), the central-like VPC-based sum rate maximization problem to be solved by BS  $i$  can be written as

$$\max_{\mathbf{Z}_i, \mathbf{P}_\ell} R_i(\mathbf{Z}_i, \mathbf{P}_\ell) \quad (16a)$$

$$\text{s.t. } \text{Tr}(\mathbf{Z}_i \mathbf{Z}_i^H) \leq P_{\max}, \quad (16b)$$

$$\text{Tr}(\mathbf{P}_\ell \mathbf{P}_\ell^H) \leq P_{\max}, \forall \ell \neq i, \quad (16c)$$

which can be solved by the WMMSE method [137].

It is noted that, by the VPC-based scheme, only the interference channels and the transmission powers are required to be exchanged between the BSs. Since these two terms are not related to the number of transmit antennas, the backhaul cost of the VPC-based scheme is relatively low, especially for the ELAA systems where the transmit antenna is large.



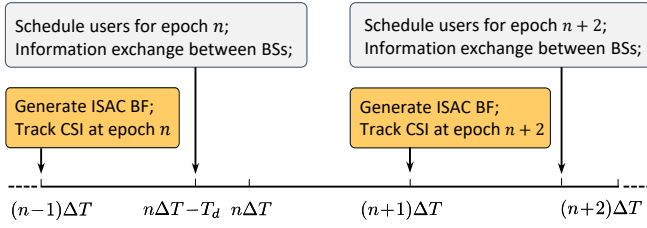


Fig. 7: Illustrations of the ISAC-based distributed user scheduling and beamforming design framework.

3) *Sensing-Assisted Distributed User Scheduling*: Distributed user scheduling with the merits of distributed processing also plays an important role to improve the network spectral efficiency while incurring a low backhaul cost [145], [149], [150]. For most existing distributed algorithms, including that discussed in the previous subsection, the CSIs or inter-cell interference powers are still required to be periodically exchanged between the BSs in each iteration of the algorithm. However, in time-varying environments, frequent message exchanges will cause extra delays, and the BSs would have outdated information. The SLINR-based scheme, which only needs the intra-cell interference and the leakage to users in other cells, is an efficient way to alleviate this issue [137], [146]. However, the coupling of user scheduling variables in the SLINR term causes the difficulty of estimating the cross-cell leakage. The work [145] further introduced a traffic model to estimate the leakage approximately without requiring knowing the scheduling variables of other cells. However, the traffic model in [145] cannot offer real-time leakage estimate, which can cause a discrepancy between SLINR and the true SINR, degrading the performance in dynamic environments.

To address these challenges, [151] proposed an ISAC-based distributed user scheduling and beamforming design framework that can provide close-to-centralized performance with significantly reduced information exchange overhead. In particular, as shown in Fig. 7, [151] considered a transmission time  $T$ , which is divided into  $N$  equal-length epochs, and the length of each is  $\Delta T$ . Based on this setting, the proposed ISAC-based distributed user scheduling and beamforming design framework consists of four steps in each epoch:

- i) **ISAC Signal Transmission**: At time  $(n-1)\Delta T$ , each BS transmits the data signal with ISAC beamformers. Based on the reflected signal, each BS can obtain the estimated kinematic parameters and the corresponding channel estimate of the served users;
- ii) **Per-cell Scheduling**: At time  $(n\Delta T - T_d)$ , by utilizing the estimated channel, each BS conducts a user scheduling scheme to determine the scheduled user set for epoch  $n$ .
- iii) **Information Exchange**: After computing the coordinates of scheduled users from the angle and distance information, each BS exchanges their coordinates and velocity information to other BSs, which will be used by other BSs to estimate its cross-cell LoS channel.
- iv) **Distributed ISAC Beamforming**: At time  $n\Delta T$ , with the channel estimates of its served users and its cross-cell channels, each BS optimizes ISAC transmit beamformers

by solving a sum rate maximization problem.

This scheme can adaptively track the users' kinematic parameters in a dynamic environment and realize accurate channel estimation, enabling high-quality user scheduling and beamforming designs. Besides, this scheme also avoids the need for extensive CSI exchanges between BSs, thereby reducing the backhaul cost.

There exist several interesting directions for future research. First, improving sensing performance in scenarios where line-of-sight (LoS) channels are unavailable is essential. Such environments, including urban canyons or indoor settings, require advanced sensing techniques that can effectively utilize non-LoS signals, for accurate user localization. Second, developing robust distributed user scheduling and beamforming algorithms that account for sensing errors is equally important. These algorithms should be capable of maintaining high network performance and mitigating the adverse effects of inaccuracies in sensing data, ensuring reliability in dynamic and challenging environments.

### C. Distributed SP for CF-mMIMO System

In the considered CF-mMIMO system, a CPU coordinates  $C$  multi-antenna APs to cooperatively serve  $K$  users in a certain area. The CF-mMIMO system has a quite similar architecture to the single-BS ELAA system using a star-networked DBP architecture, except for that the APs (can be viewed as DNs) are spatially distributed. Then, it depends on the functional split between CPU and APs with options ranging from 7.2 and 8 in [152] to fully distributed in [153].

In functional split option 8, the processing down to the baseband signal is performed in the CPU. The APs only perform RF processing and transmit (receive) the pure sampled and quantized baseband signals to (from) the CPU via fronthaul links. Therefore, option 8 has the lowest processing power requirements of the APs. However, the rate requirements of the fronthaul links are high. Lower fronthaul requirements has option 7.2. Low PHY functions are implemented at the AP. Joint processing can still be performed at the CPU while the complexity of the APs is kept low. In contrast, the fully distributed functional split architecture in [153] implements both high and low PHY functions. One speciality is the option to control lower PHY functions of several cluster APs by one high PHY function in one cluster head AP.

Distributed SP is important for CF-mMIMO system for improving the system scalability [154]–[156]. The work [154] investigates uplink equalization problem in the CF-mMIMO system and proposes three distributed algorithms based on linear equalizers, which only requires the DNs to send low-dimensional signals (e.g., the local estimates) to the CN for fronthaul reduction. The works [155], [156] study the distributed downlink precoding problem in CF-mMIMO systems. The complexity of the CF-mMIMO system scales rapidly with the network size. To address this issue, user-centric CF-mMIMO systems with user-AP association have been proposed, which improve the system scalability [157], [158].

It depends on the constraints of fronthaul and midhaul links, whether the signal processing, such as channel estimation, pre-

and de-coding, equalization, modulation and demodulation, coding and decoding, can be performed in a centralized or de-centralized manner. For the uplink transmission, the signal processing for MMSE and maximum likelihood in the uplink can be performed decentralized without loss of optimality [159]. There, it is shown that in the sequential processing [159, Algorithm 1] the estimate obtained at one AP is equivalent to that obtained by centralized processing with LMMSE receiver. For the downlink, the team precoding framework in [160] allows an optimal distributed spatial pre-coding and power control.

The main challenge in CF-mMIMO is to achieve the benefits of cell-free operation in a practical way, with computational complexity and fronthaul requirements that are scalable to enable massively large networks with many mobile devices [161]. The monograph [161] describes the state-of-the-art signal processing algorithms for channel estimation, uplink data reception, and downlink data transmission with either centralized or distributed implementation.

Recently, the work [162] investigated the distributed resource allocation for a user-centric CF-mMIMO system, where two distributed algorithms are proposed to jointly optimize the user association and precoding. The SLNR-based metric is also applied for backhaul signaling reduction. In [163], a joint optimization of fronthaul load and computation resources in CF-mMIMO networks is performed. It is one of the first papers to consider a graph model for the fronthaul network jointly with the cell-free wireless access.

The relation between CF-mMIMO and Open-RAN together with a review of next generation multiple access methods is provided in [164].

1) *Future Work*: CF-mMIMO has received significant attention from the signal processing perspective. In particular, the distributed channel estimation and signal detection both for up- and downlink were studied in detail [165]. However, the constraints and requirements from the fronthaul network leave several open research questions for future work.

What is the optimal choice of the functional split and corresponding distributed signal processing given fronthaul constraints and user rate requirements? Since demands and requirements are time variant, a flexible functional split would help to improve the efficiency [166]. Enhanced coding schemes, such as rate-splitting can lower the fronthaul requirements and improve the achievable rates in CF-mMIMO [167].

What is the impact of impairments in the fronthaul links and the RF-chains at the APs? How can we develop robust precoding and resource allocation schemes which are resilient against impairments and faults on the fronthaul and wireless links? The effects of dirty RF, such as phase noise, on the performance of CF-mMIMO is studied in recent works [168]. Severe fronthaul limitations are considered in [169], and robust receivers are developed.

How can a deployment of CF-mMIMO establish near-field beamforming gains and high localization precision? In [170], the near-field MIMO communications is motivated by CF-mMIMO among others. Depending on carrier frequencies and antenna as well as AP spacing, user terminals in the near-field can enjoy highly directive and selective receive signal powers.

## V. DISTRIBUTED SP FOR ELAA SYSTEMS INTEGRATED WITH EMERGING TECHNOLOGIES

Recently, there has been a growing trend to integrate emerging technologies into ELAA systems to further enhance system performance. These integrations aim to improve spectral efficiency, expand wireless coverage, and enable new functionalities such as wireless sensing. In this section, we explore the interplay between ELAA systems and several key emerging technologies. Specifically, we focus on four prominent technologies: repeater-assisted multi-user MIMO, backscatter communication, RIS, and ISAC. We will delve into the advantages these integrations offer and examine the potential trade-offs and challenges they introduce.

### A. Repeater-Assisted Multi-User MIMO

Cellular-massive-MIMO [33], the backbone of the 5G physical layer, is a very powerful technology. But coverage holes, and difficulties to send multiple streams to multi-antenna users because of insufficient channel rank, remain issues. The ultimate solution will be distributed and extremely-large scale MIMO, but while these are at heart strong technologies, installing fronthaul and backhaul can be expensive, and achieving accurate phase-alignment for coherent multiuser beamforming on downlink remains a difficult technical problem (see Section III-E).

Ways of improving performance by *augmenting the propagation environment* with new paths are therefore desirable. One option is to deploy RISs [171], [172] – but they have large, perhaps unrealistically large, form factors and require significant amounts of training and control overhead. Also, probably, in practice, some form of active filtering is required to make them sufficiently band-selective.

A different, radically new approach is to deploy large numbers of physically small and cheap wireless repeaters, that receive and instantaneously retransmit signals – appearing as if they were ordinary scatterers in the channel, but with amplification [173]. Repeaters, as such, are deployed today already but only in niche use cases (for example, in tunnels). Could they be deployed at scale, in swarms, within the cells? What would be required of the repeaters, and how well could a repeater-assisted cellular massive MIMO system work, compared to distributed MIMO? What are the fundamental limits of this technology?

Among several different possible designs, the most promising one is dual-antenna repeaters that switch between two separate amplification paths (one path from a first to a second antenna, and one path from the second antenna to the first), in alignment with the TDD pattern. Such repeaters can, with appropriate calibration [174], be made *reciprocal*, such that they appear *transparently* to the network as channel scatterers with amplification. In particular, this makes reciprocity-based multiuser MIMO beamforming [33] work, by relying on uplink channel estimates for the downlink beamforming. This way, the repeater can do the job of a RIS but with essentially no control overhead, and a two-order-of-magnitude smaller form factor.

An important consideration when deploying repeater swarms within a cell is that depending on the repeater amplification levels, the repeaters will mutually interfere and amplify the signals transmitted by each other. One must ensure that the amplification levels are set such that the positive feedback loops created between the repeaters are stable (within an appropriate safety margin). Optimal configuration of repeater swarms under such constraints is an open problem; some initial analysis from a control-theoretic viewpoint can be found in [175].

Another open problem is to optimize power allocation and receiver algorithms to minimize the effects of amplified noise. Repeaters, being active devices with power amplifiers, will introduce thermal noise that gets amplified and transmitted, and received at the base station arrays. This noise can be mitigated, and amplification levels and activation strategies can be optimized to minimize its impact.

As demonstrated in [173], repeater-assisted cellular MIMO could approach distributed-MIMO performance, but with much simpler deployments that require no backhaul and no phase alignment. There are significant opportunities to innovate new solutions within this nascent area of physical-layer wireless research.

### B. Backscattering Communications

Energy-neutral wireless devices, also sometimes known as “passive” devices, do not have a battery but rely on harvesting of radio-frequency power for their operation. These devices communicate through backscattering and do not have a conventional radio-frequency frontend, but only an antenna whose load impedance can be controlled. By controlling this impedance, the device can change the phase of the wave scattered from its antenna when illuminated with an incoming wave. There are three main architectures for backscattering communication: (a) In a monostatic setup, the transmitter and receiver are co-located and share the same antenna arrays [176]–[178]; such systems require full-duplex technology at the arrays. (b) In a bistatic setup, the transmitter and receiver are spatially separated and do not share circuitry [179], [180]; full-duplex technology is not required. (c) An ambient backscattering system does not have a dedicated transmitter but relies on ambient radio sources such as Bluetooth, WiFi, or TV broadcast signals [181].

The bistatic setup has the largest potential and integrates naturally with extremely large arrays distributed MIMO, with pairs of MIMO panels acting as transmitter and receiver.

The received backscattered signal is typically weak compared to the direct link between the transmitter and receiver. This requires a high dynamic range of reader circuitry [182], mitigation techniques [183], [184] or the use of advanced beamforming techniques to suppress direct link interference [185]. Direct link interference cancellation for bistatic setups brings several new elements: for example, there can be a carrier frequency or phase offset between the panels [186]. In addition, these panels are not necessarily synchronized in phase (cf. Section III-E).

The service of energy-neutral (passive) devices is challenging owing to the poor link budget: the path gains from the

transmitter to the device and from the device to the receiver multiply. This requires sensitive and efficient signal processing algorithms. Some specific, new problems that emerge are:

**i) Robust beamforming for initial access:** In practice, when beamforming to a passive device, only a rough estimate of the channel may be available. For example, the channel could be estimated at some point in time, but be outdated. The question then arises as to how beamforming could be made more robust: rather than sending a single beam obtained from the outdated channel estimate, could several beams be formed whose combined action provide sufficient power to the device?

One may, for example, employ beam diversity [187]. More sophisticatedly, suppose we have access to an estimate of the channel response, say  $\mathbf{g}$ , at a nominal focal point. Suppose in addition that we could predict how this channel response varies within some neighborhood of that nominal focal point, and that we take samples from this neighborhood. Such prediction could be performed, for example, by exploiting a geometric model. Alternatively, it could be based on historical channel state information, by constructing a database of past impulse responses stored in chronological order, forming a *data-driven parameterization* of a neighborhoods around nominally measured channel responses.

In a nutshell, the problem is to find a beam  $\mathbf{w}$  that maximizes  $\min_i |\mathbf{g}_i^H \mathbf{w}|$ , given channel vectors  $\{\mathbf{g}_i\}$  sampled from the neighborhood. This problem is reminiscent of multicast beamforming and can be cast as a maximin matrix optimization problem. For example, one can write  $\mathbf{X} = \mathbf{w}\mathbf{w}^H$  (rank-one) and minimize  $\|\mathbf{w}\|^2 = \text{Tr}\{\mathbf{X}\}$  subject to constraints of the form  $|\mathbf{w}^H \mathbf{g}_i|^2 = \text{Tr}\{\mathbf{X} \mathbf{g}_i \mathbf{g}_i^H\} > \text{threshold}$  for all  $i$  by relaxing the rank constraint on  $\mathbf{X}$  into a semidefiniteness constraint; once  $\mathbf{X}$  is found, keep its principal eigendirection. A next question is how to obtain *multiple beamvectors*  $\{\mathbf{w}_k\}$  such that  $\min_i \max_k |\mathbf{g}_i^H \mathbf{w}_k|$  is large. (If the device has a large enough supercapacitor, the relevant objective would instead be  $\min_i \sum_k |\mathbf{g}_i^H \mathbf{w}_k|$ .) Some initial results on data-driven algorithms for this are given in [188].

**ii) Beamforming with direct-link interference suppression:** Algorithms must be developed that can obtain (partial) channel state information to the device and beamform towards it, at the same time as direct link interference is suppressed. For example, for the bistatic distributed MIMO setup, one can transmit into the nullspace of an estimated channel between the transmitting and receiving panels [185], thereby reducing direct link interference.

**iii) Panel selection and integration into the TDD flow:** For communication with a backscattering device, a subset of [antenna] panels needs be designated as transmitters and another subset as receivers [189]. One approach is to quantify the prior knowledge of the location (channel) of the backscattering device via a probability distribution that can be learned and tracked over time, and then find the panel assignment that maximizes the worst-case, or average, performance over this distribution. Furthermore, communication with a backscattering device requires breaking the nominal TDD flow, which calls for dynamic and flexible duplex access operation patterns.

### C. ELAA with RIS

Reconfigurable intelligent surfaces (RIS) are surfaces which can be electronically controlled to change their electromagnetic reflection properties [190]. Thereby, the channel properties can be adapted to the requirements of the communication system, e.g., to improve the scaling with the number of antennas, reduce the transmit power with number of RIS elements [191], enlarge the coverage region [192], [193], and etc.

The main difference of the RIS-assisted signal model to the one presented in Section III is that the new channel matrix  $\tilde{\mathbf{H}}_i$  in (1) contains the contributions of the direct link  $\mathbf{H}_i$  and the contributions from the reflection of the RIS  $\mathbf{G}\Theta\mathbf{F}_i$  with channel matrix  $\mathbf{F}_i$  from the  $i$ -DN to the RIS and channel matrix  $\mathbf{G}$  from the RIS to the user. The matrix  $\Theta$  describes the operation at the RIS and its structure and its constraints depend on the RIS technology applied. The overall channel from the DN  $i$  to one user is given by

$$\tilde{\mathbf{H}}_i = \mathbf{H}_i + \mathbf{G}\Theta\mathbf{F}_i. \quad (17)$$

The classical constraint sets of the RIS matrix  $\Theta$  is the diagonal matrix with unit modulus entries corresponding to phase shifts of each RIS element. Under this constraint, the design of RIS assisted multi-cell transmission systems is considered in [194], [195]. To support the connectivity of users in blind areas while ease the CSI acquisition overhead at each DN, statistical CSI based transmission design is a reasonable choice. With only statistical CSI at both the DNs and the RIS, it is obtained that the statistical maximum ratio transmission beamforming is almost optimal at each DN. This allows each DN to design the beamforming vectors of their own independently, which greatly reduces the design complexity. Moreover, the RIS phase shift design is also decoupled with the DNs' beamforming design. Besides the unit modulus constraint, discretized diagonal RIS models exists, where only a certain number of equidistant phases are supported [196], [197]. More recently, the beyond-diagonal RIS model is introduced, where circuitry allows to transfer received signals between RIS elements [198]. The constraint set in this case correspond to symmetric and unitary matrices

$$\Theta = \Theta^T \quad \text{and} \quad \Theta^H \Theta = \mathbf{I}. \quad (18)$$

In the single-user scenario for one DNs, for fixed transmit  $\mathbf{w}_i$  and receive beamforming  $\mathbf{v}$ , the resulting RIS optimization problem can be cast as

$$\max_{\Theta \text{ fulfills (18)}} |\mathbf{v}^H \mathbf{H}_i \mathbf{w}_i + \mathbf{v}^H \mathbf{G}\Theta\mathbf{F}_i \mathbf{w}_i|^2, \quad (19)$$

which can be solved in closed form by exploiting the Takagi factorization as explained in [199]. In the case with multiple DNs, the optimization problem is more difficult

$$\max_{\Theta \text{ fulfills (18)}} \sum_{i=1}^C |\mathbf{v}^H (\mathbf{H}_i + \mathbf{G}\Theta\mathbf{F}_i) \mathbf{w}_i|^2. \quad (20)$$

The programming problem in (20) is difficult because the sum cannot be easily decomposed and  $\Theta$  cannot be separated.

For the multi-user MIMO case, the effective channel for user  $k$  in the downlink from  $C$  DNs can be written as

$$\tilde{\mathbf{H}}_{i,k} = \sum_{i=1}^C (\mathbf{H}_{i,k} + \mathbf{G}_k \Theta \mathbf{F}_i), \quad (21)$$

and the achievable rate expression for user  $k$  reads as in (14) with the difference that the effective channels contain contributions from the RIS. For the classical setup of MCP precoding with RIS optimization, the model and programming problem is formulated in [200].

The joint optimization of transmit covariance matrices and RIS-elements is performed in combination with next generation multiple access technologies, namely NOMA in [201] and rate splitting multiple access (RSMA) in [202]. For simultaneous transmission and reflection (STAR) RIS configuration, the corresponding model and problem are formulated and solved in [203].

In [204], RIS-assisted CF-mMIMO transmission over spatially correlated channels is optimized. An asymptotic analysis of the performance for growing number of APs and RIS elements is performed. The performance benefits of using RISs in CF-mMIMO systems are confirmed.

There are several open questions and topics for future research. First of all, the optimization of the RIS elements for different constraint sets including diagonal, BD-, STAR-RIS, globally passive, partly active under distributed massive MIMO has open challenges. If discrete constraint sets for the RIS elements are considered, tools and methods from discrete optimization need to be applied.

Second, in many scenarios the RIS should be placed either close to the transmitter or to the receiver, if it is totally passive [205]. Then, it will operate most likely in the near-field of the corresponding transmitter or receiver. The resulting effect channel is then a quintuple  $\mathbf{R}\Phi\mathbf{H}\Theta\mathbf{T}$ , where the channel from the transmitter to the first RIS is denoted by  $\mathbf{T}$ , the channel from first RIS to second RIS by  $\mathbf{H}$ , and the channel from the receiver RIS to the receiver by  $\mathbf{R}$ . The two RIS matrices are denoted by  $\Phi$  and  $\Theta$ . A joint optimization of  $\Phi$  and  $\Theta$  remains an interesting problem.

### D. ELAA with ISAC

The future of ISAC systems will witness a profound fusion of communication and sensing capabilities, evolving from hardware, spectrum, and functional integration to a state of mutual benefit, high coordination, and deep integration [206]. 6G networks transcend the limitations of single-BS and single-UE perception, adopting an inherent sensing design across network architecture, networking technologies, and air interface capabilities to achieve high-precision perception. Leveraging the 6G network, collaborative sensing technologies will emerge as a key component of ISAC system. This technology enhances the user experience at the edge and enables high-resolution sensing of multiple targets [207]–[209]. Collaborative sensing involves the cooperation and interaction of nodes within the mobile communication network, including large-scale deployed BS nodes and densely distributed UE nodes. By utilizing multiple nodes for receiving

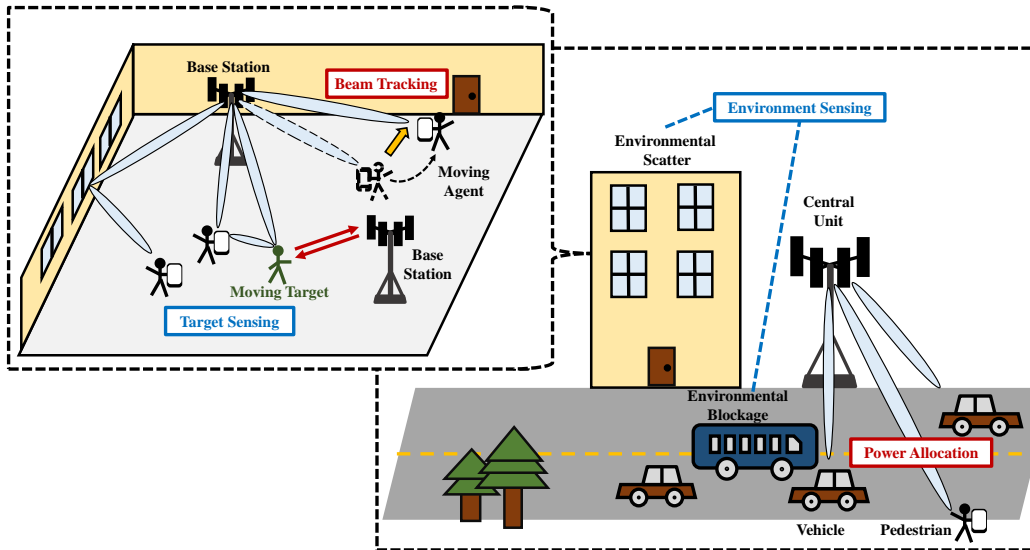


Fig. 8: ELAA-enabled ISAC functions in distributed systems.

and transmitting sensing signals, collaborative sensing avoids the self-interference issues inherent in single-node perception, reducing the demand for receiver self-interference cancellation capabilities and lowering hardware costs.

ELAA systems are inherently suited for ISAC due to their shared hardware resources and similar signal processing methods. As for sensing, the same antenna array used for transmitting and receiving communication signals can also be utilized for sensing by analyzing the reflected echoes or the communication pilots. ELAA-enabled ISAC unlocks significant advantages in terms of performance. The ability of ELAA to realize precise beamforming translates to increased spatial resolution and effective range for sensing services, which brings about high-resolution UE localization and high-resolution environmental map construction [210], [211].

For communication, ELAA-enabled ISAC enables highly targeted data transmission with minimal interference in multiple UE scenarios. The spatial awareness offered by ELAA sensing capabilities can be used to optimize resource allocation, scheduling, and interference management across multiple UEs and BSs. For instance, by sensing the movements of multiple UEs and the environmental maps [212], [213], an ELAA-enabled ISAC system can dynamically adjust beamforming patterns and allocate resources to maximize throughput and minimize interference. Similarly, in a multi-BS setup [214], sensing data can facilitate coordinated beamforming and interference mitigation strategies among BSs, leading to a more efficient and robust network. Furthermore, joint signal processing techniques can leverage information from both sensing and communication tasks to improve overall system performance by optimizing metrics of joint design. The ISAC functions in ELAA systems are shown in Fig. 8, with sensing functions in blue, and communication functions in red.

Despite the considerable potential, several challenges remain in realizing the full potential of ELAA-enabled ISAC. Efficient power allocation and interference management are crucial to ensure both functionalities operate optimally with-

out compromising each other. The design of sophisticated joint signal processing algorithms that effectively exploit the synergy between sensing and communication data is another significant challenge. Additionally, the hardware complexity and associated costs of implementing ELAA systems with a large number of antenna elements can be substantial and require further research and development for cost-effective solutions. ELAA-enabled ISAC in distributed systems holds immense promise for revolutionizing various fields. By addressing the remaining challenges and continuing to innovate in this domain, we can unlock the full potential of this transformative technology and create a future where sensing and communication seamlessly coexist and augment each other.

## VI. OUTLOOK FOR FUTURE DIRECTIONS

In this section, we outline several important future research directions that are essential for improving the performance and practicality of ELAA systems.

### A. Distributed SP for ELAA in the Near Field

In addition to fronthaul cost and computational complexity bottlenecks, ELAA systems face unique challenges due to the extremely large number of antennas operating in the radiating near-field region. Unlike conventional wireless systems functioning in the far-field, near-field communications fundamentally alter the electromagnetic field properties. Two key phenomena emerge in this context: spatial nonstationarity and spherical wavefronts. Spatial nonstationarity means different parts of the antenna array may experience the same channel paths with varying power or entirely different channel paths, while spherical wavefronts account for the curvature of signal propagation due to closer proximity between transmitter and receiver [45], [46].

These phenomena present both challenges and opportunities for signal processing. For instance, near-field effects complicate channel estimation and beamforming but also offer enhanced spatial degrees-of-freedom and improved interference



mitigation capabilities. Existing studies have explored these complexities: spatial nonstationarity-focused channel estimation has been examined in [215], spherical wavefront channel estimation in [216], and joint investigations of both phenomena in [217]. Additionally, [218]–[220] demonstrated that precise downlink beamforming leveraging these effects could enable focused beams, providing a novel degree of freedom to reduce multiuser interference.

To fully exploit the potential of near-field ELAA systems, innovative distributed SP algorithms are necessary. Unlike in far-field systems, where DBP architectures rely on pre-configured antenna clusters, near-field spatial nonstationarity calls for dynamic clustering approaches. Such methods could optimize antenna utilization by identifying and leveraging sparsity patterns in the antenna-domain channel. Furthermore, spherical wavefronts present new opportunities for enhancing both communication and localization, necessitating distributed algorithms that are specifically designed to account for curvature effects in wave propagation.

Finally, while addressing these technical issues, it is critical to consider practical deployment scenarios. The susceptibility of near-field ELAA systems to interference from nearby scatterers and the challenges of maintaining synchronization among distributed nodes further emphasize the importance of robust and efficient algorithmic designs. Future research should prioritize developing SP algorithms that balance these challenges with the unprecedented advantages of near-field ELAA systems.

### B. ELAA Realizations with Flexible Antennas

The development of ELAA systems is poised to benefit significantly from advancements in antenna technologies. Incorporating novel antenna designs can further enhance the performance and flexibility of ELAA systems. Recently, several advanced antenna techniques have emerged, such as fluid antennas [221] and movable antennas [222]. Unlike conventional antenna techniques, where antennas are fixed in position, these new technologies allow for flexible adjustment of antenna positions within a spatial region [223]–[227]. With flexible antenna positions, the system can dynamically adapt to changing environments, providing more consistent channel conditions to enhance the received signal power. However, in these flexible-antenna systems, the movement of antennas is typically constrained to the scale of the wavelength, which limits their impact on large-scale path loss and restricts their applicability in various scenarios.

More recently, the pinching antenna has emerged as a more promising solution to address the limitations of conventional flexible antenna systems [228], [229]. Unlike the other flexible antenna systems, pinching antennas utilize a dielectric waveguide as the transmission medium, allowing for dynamic activation at any point along the waveguide by adding or removing separate dielectric materials. This innovation enables much greater flexibility in antenna deployment. Additionally, compared to traditional flexible antennas, pinching antennas are more cost-effective and simpler to install, as their functionality is achieved through the straightforward process of

adding or removing dielectric materials. These advantages make pinching antennas particularly well-suited for environments where adaptability and cost-efficiency are key, such as in industrial Internet of Things (IoT) applications or urban deployments.

While these new flexible antenna technologies offer significant promise, they also introduce new research challenges. Developing efficient algorithms to control and optimize flexible antennas, ensuring seamless integration with existing network infrastructure, and addressing potential cost and complexity issues are critical areas for future research. Additionally, investigating the impact of these technologies on network performance, user experience, and overall system reliability will be essential to realize their full potential.

### C. ELAA for Physical Layer Security

Physical layer security (PhySec) refers to algorithms and schemes which exploit physical parameters and properties of the transceiver as well as the wireless channel to obtain security primitives. This is considered as the first line of defense for 6G wireless communication networks [230].

ELAA can support PhySec schemes, like, e.g., wiretap coding, secret key generation, and authentication. Due to the distributed large number of transmit antennas, the beamforming can focus the energy towards the intended receivers while reducing information leakage to eavesdroppers. The remaining information leakage is handled by wiretap coding. Following the signal model for the ELAA downlink precoding from (8) for the case with one sub-carrier, the sum secrecy rate maximization problem for confidential data transmission reads as follows

$$\max_{\{\mathbf{Z}_{i,k}\}} \sum_{k=1}^K SR_k \quad \text{s.t.} \quad (9b), \quad (22)$$

where  $SR_k = [R_k - R_\ell]^+$  is the achievable secrecy rate. It is equal to the achievable rate of user  $k$  minus the achievable rate to the eavesdropper  $\ell$ . While for single-user, the global optimal precoding is known [231], for the multi-user case only algorithms to achieve the stationary solution exist [232]. For CF-mMIMO, the physical layer secrecy is optimized for downlink transmission in [233]. Very recently, PhySec with near-field beamforming is introduced in [234]. For secret key generation (SKG) in multi-carrier MIMO networks exists efficient and robust solutions [235] also against various attacks. SKG in downlink massive MIMO is studied in [236]. However, SKG algorithms that takes the constraints and properties of the ELAA systems into account are not available yet.

The wireless fingerprints, which are essentially the measured effective channels between the transmitter and receiver [237], contain more information as the number of antennas increases [238]. For the CF-mMIMO architecture, [239] studies user location estimation method based on fingerprint positioning. Important aspects are the careful selection of the AP and corresponding local channel estimation.

### D. Low-Resolution Designs for ELAA Systems

Recent research on multi-antenna systems has shown substantial interest in techniques related to low-resolution or

coarsely quantized signals from a fundamental signal processing perspective [240]–[244]. This trend is driven by the potential to replace high-resolution analog-to-digital converters (ADCs) and digital-to-analog converters (DACs) with lower resolution alternatives, particularly the very cheap one-bit ADCs/DACs [243], [244]. Utilizing such low-resolution schemes can significantly reduce the hardware complexity and power consumption of radio-frequency front ends. For ELAA systems, low-resolution designs become even more critical because the number of ADCs/DACs and radio-frequency front ends needs to scale proportionally with the very large number of antennas. Consequently, addressing issues related to hardware cost and energy consumption is crucial, as these could otherwise become prohibitively expensive in ELAA systems.

There have been numerous studies exploring low-resolution designs in massive MIMO systems. For example, [243], [245], [246] investigated the one-bit channel estimation problem in massive MIMO systems. The impact of coarse quantization on channel estimation accuracy and achievable rate was studied in [243], and efficient channel estimation algorithms were developed based on Gaussian latent models in [245]. One-bit precoding designs, using criteria such as MMSE and minimum symbol error probability, have been explored in [247], [248]. Another important challenge is uplink MIMO detection with low-resolution ADCs/DACs. The research in [249] explored the application of linear receivers in the low-resolution scenario, while maximum likelihood-based detectors were investigated in [250]–[252].

While these low-resolution schemes have demonstrated promising numerical performance, there are significant challenges. The primary difficulty lies in the development of efficient non-convex algorithms that can handle large-scale binary optimization problems. Such algorithms are critical for making ELAA systems practical, particularly when addressing the need for high-performance while keeping hardware and computational costs low. Additionally, low-resolution designs inherently introduce trade-offs, particularly in terms of channel estimation accuracy, signal-to-noise ratio (SNR), and system capacity. Although they can reduce hardware complexity, they also tend to degrade system performance due to quantization errors. This makes it crucial to find a balance between cost savings and performance loss. Future research should focus on strategies to mitigate these trade-offs, possibly by developing hybrid ADC/DAC systems or advanced signal processing techniques that minimize the impact of quantization errors.

#### E. ELAA for Satellite Communications

Satellite communications (SATCOM) are expected to play a pivotal role in the future wireless ecosystem, especially in providing global coverage for remote and underserved areas. As demand for high-speed, low-latency communication continues to rise across industries like the Internet of Things (IoT), autonomous systems, and disaster recovery, SATCOM must evolve to meet the demands of the 6G era [253]. Recent advances have demonstrated that the application of ELAA (in the form of distributed MIMO) technologies to SATCOM is emerging as a promising solution for improving system performance, capacity, and coverage [254], [255].

The use of ELAA systems in SATCOM offers several unique advantages. By deploying large numbers of antennas on both the satellite and ground stations, ELAA systems can significantly enhance beamforming precision, thereby mitigating interference, improving signal coverage, and increasing capacity, especially in high-user-density environments or areas with challenging propagation conditions. However, the deployment of ELAA systems in SATCOM also introduces substantial challenges. The large size and complexity of antennas required for ELAA can increase costs and pose challenges in satellite payload design. Additionally, the need for precise beamforming and the handling of large-scale antennas in space introduces significant technical complexity [256]. Furthermore, the integration of ELAA systems with terrestrial networks and overcoming the inherent latency of satellite communications require advances in distributed SP algorithms to ensure seamless and efficient operation.

Despite these challenges, ELAA for SATCOM presents significant potential to enhance system performance and is an important research area for the next-generation communication systems. Addressing the technical challenges associated with large-scale antenna integration, beamforming, and distributed SP will be critical for realizing the full potential of ELAA in SATCOM for next-generation wireless communications.

## VII. CONCLUSION

ELAA systems are crucial for realizing the full potential of 6G wireless communication networks. As the number of antennas in ELAA systems increases, significant challenges such as excessive interconnection costs and high computational complexity emerge. Efficient distributed SP algorithms have shown great promise in addressing these challenges. We began by presenting three representative forms of ELAA systems: single-BS ELAA systems, coordinated distributed antenna systems, and ELAA systems integrated with emerging technologies. For each form, we reviewed the associated distributed SP algorithms designed to mitigate the bottlenecks. Additionally, we highlighted several important future research directions, including distributed SP algorithm design in the near-field, low-resolution design for ELAA systems, ELAA for physical layer security, and the incorporation of advanced antenna technologies. Addressing these areas is essential for further improving the performance and practicality of ELAA systems. In conclusion, while significant progress has been made in the development of distributed SP algorithms for ELAA systems, ongoing research and innovation are still required to overcome existing challenges and fully realize the potential of ELAA in next-generation wireless networks.

## REFERENCES

- [1] E. Björnson, Y. C. Eldar, E. G. Larsson, A. Lozano, and H. V. Poor, "Twenty-five years of signal processing advances for multiantenna communications: From theory to mainstream technology," *IEEE Signal Process. Mag.*, vol. 40, no. 4, pp. 107–117, 2023.
- [2] E. G. Larsson, O. Edfors, F. Tufvesson, and T. L. Marzetta, "Massive MIMO for next generation wireless systems," *IEEE Commun. Mag.*, vol. 52, no. 2, pp. 186–195, 2014.
- [3] L. Lu, G. Y. Li, A. L. Swindlehurst, A. Ashikhmin, and R. Zhang, "An overview of massive MIMO: Benefits and challenges," *IEEE J. Sel. Top. Signal Process.*, vol. 8, no. 5, pp. 742–758, 2014.

- [4] A. B. Gershman, N. D. Sidiropoulos, S. Shahbazpanahi, M. Bengtsson, and B. Ottersten, "Convex optimization-based beamforming," *IEEE Signal Process. Mag.*, vol. 27, no. 3, pp. 62–75, 2010.
- [5] Z.-Q. Luo, W.-K. Ma, A. M.-C. So, Y. Ye, and S. Zhang, "Semidefinite relaxation of quadratic optimization problems," *IEEE Signal Process. Mag.*, vol. 27, no. 3, pp. 20–34, 2010.
- [6] J. G. Andrews, S. Buzzi, W. Choi, S. V. Hanly, A. Lozano, A. C. Soong, and J. C. Zhang, "What will 5G be?" *IEEE J. Sel. Areas Commun.*, vol. 32, no. 6, pp. 1065–1082, 2014.
- [7] E. Perahia and R. Stacey, *Next generation wireless LANs: 802.11 n and 802.11 ac*. Cambridge university press, 2013.
- [8] E. Khorov, A. Kiryanov, A. Lyakhov, and G. Bianchi, "A tutorial on IEEE 802.11 ax high efficiency WLANs," *IEEE Commun. Surv. Tutorials*, vol. 21, no. 1, pp. 197–216, 2018.
- [9] L. You, K.-X. Li, J. Wang, X. Gao, X.-G. Xia, and B. Ottersten, "Massive MIMO transmission for LEO satellite communications," *IEEE J. Sel. Areas Commun.*, vol. 38, no. 8, pp. 1851–1865, 2020.
- [10] O. Kodheli, E. Lagunas, N. Maturo, S. K. Sharma, B. Shankar, J. F. M. Montoya, J. C. M. Duncan, D. Spano, S. Chatzinotas, S. Kisseleff *et al.*, "Satellite communications in the new space era: A survey and future challenges," *IEEE Commun. Surv. Tutorials*, vol. 23, no. 1, pp. 70–109, 2020.
- [11] J. Heo, S. Sung, H. Lee, I. Hwang, and D. Hong, "MIMO satellite communication systems: A survey from the PHY layer perspective," *IEEE Commun. Surv. Tutorials*, 2023.
- [12] J. Li and P. Stoica, "MIMO radar with colocated antennas," *IEEE Signal Process. Mag.*, vol. 24, no. 5, pp. 106–114, 2007.
- [13] S. H. Talisa, K. W. O'Haver, T. M. Comberiate, M. D. Sharp, and O. F. Somerlock, "Benefits of digital phased array radars," *Proc. IEEE*, vol. 104, no. 3, pp. 530–543, 2016.
- [14] E. Björnson, Y. C. Eldar, E. G. Larsson, A. Lozano, and H. V. Poor, "Twenty-five years of signal processing advances for multiantenna communications: From theory to mainstream technology," *IEEE Signal Process. Mag.*, vol. 40, no. 4, pp. 107–117, 2023.
- [15] G. J. Foschini and M. J. Gans, "On limits of wireless communications in a fading environment when using multiple antennas," *Wireless Pers. Commun.*, vol. 6, pp. 311–335, 1998.
- [16] E. Telatar, "Capacity of multi-antenna gaussian channels," *Eur. Trans. Telecommun.*, vol. 10, no. 6, pp. 585–595, 1999.
- [17] C.-N. Chuah, "Capacity scaling in MIMO wireless systems under correlated fading," *IEEE Trans. Inf. Theory*, vol. 48, no. 3, pp. 637–650, 2002.
- [18] S. M. Alamouti, "A simple transmit diversity technique for wireless communications," *IEEE J. Sel. Areas Commun.*, vol. 16, no. 8, pp. 1451–1458, 1998.
- [19] L. Zheng, "Diversity and multiplexing: A fundamental tradeoff in multiple-antenna channels," *IEEE Trans. Inf. Theory*, vol. 49, no. 5, pp. 1073–1096, 2003.
- [20] D. J. Love, R. W. Heath, and T. Strohmer, "Grassmannian beamforming for multiple-input multiple-output wireless systems," *IEEE Trans. Inf. Theory*, vol. 49, no. 10, pp. 2735–2747, 2003.
- [21] R. W. Heath, S. Sandhu, and A. Paulraj, "Antenna selection for spatial multiplexing systems with linear receivers," *IEEE Commun. Lett.*, vol. 5, no. 4, pp. 142–144, 2001.
- [22] Q. H. Spencer, A. L. Swindlehurst, and M. Haardt, "Zero-forcing methods for downlink spatial multiplexing in multiuser MIMO channels," *IEEE Trans. Signal Process.*, vol. 52, no. 2, pp. 461–471, 2004.
- [23] Y. Xu, C. Shen, Z. Ding, X. Sun, S. Yan, G. Zhu, and Z. Zhong, "Joint beamforming and power-splitting control in downlink cooperative SWIPT NOMA systems," *IEEE Trans. Signal Process.*, vol. 65, no. 18, pp. 4874–4886, 2017.
- [24] D. Tse and P. Viswanath, *Fundamentals of wireless communication*. Cambridge university press, 2005.
- [25] 3GPP, "Evolved universal terrestrial radio access (E-UTRA): Physical channels and modulation (release 8)," Technical Specification 3GPP TS 36.211, 2008.
- [26] —, "Evolved universal terrestrial radio access (E-UTRA): Multiplexing and channel coding (release 8)," Technical Specification 3GPP TS 36.212, 2008.
- [27] —, "Evolved universal terrestrial radio access (E-UTRA): Physical layer procedures (release 8)," Technical Specification 3GPP TS 36.213, 2008.
- [28] —, "Requirements for further advancements for E-UTRA (LTE-Advanced) (release 8)," Technical Report 3GPP TR 36.913, 2008.
- [29] T. L. Marzetta, "Noncooperative cellular wireless with unlimited numbers of base station antennas," *IEEE Trans. Wireless Commun.*, vol. 9, no. 11, pp. 3590–3600, 2010.
- [30] F. Rusek, D. Persson, B. K. Lau, E. G. Larsson, T. L. Marzetta, O. Edfors, and F. Tufvesson, "Scaling up MIMO: Opportunities and challenges with very large arrays," *IEEE Signal Process. Mag.*, vol. 30, no. 1, pp. 40–60, 2012.
- [31] E. Björnson, E. G. Larsson, and T. L. Marzetta, "Massive MIMO: Ten myths and one critical question," *IEEE Commun. Mag.*, vol. 54, no. 2, pp. 114–123, 2016.
- [32] L. Sanguinetti, E. Björnson, and J. Hoydis, "Toward massive MIMO 2.0: Understanding spatial correlation, interference suppression, and pilot contamination," *IEEE Trans. Commun.*, vol. 68, no. 1, pp. 232–257, 2019.
- [33] T. L. Marzetta, E. G. Larsson, H. Yang, and H. Q. Ngo, *Fundamentals of Massive MIMO*. Cambridge University Press, 2016.
- [34] C. D. Ho, H. Q. Ngo, M. Matthaiou, and T. Q. Duong, "On the performance of zero-forcing processing in multi-way massive MIMO relay networks," *IEEE Commun. Lett.*, vol. 21, no. 4, pp. 849–852, 2017.
- [35] Samsung, "Further enhancements on MIMO for NR," 3GPP RAN1, Contribution RP-202024, Feb. 2020, meeting contribution.
- [36] 3GPP, "Study on scenarios and requirements for next generation access technologies (release 16)," Technical Report 3GPP TR 38.913 V16.0.0, Jul. 2020.
- [37] —, "Physical layer procedures for data in 5G-NR," Technical Specification 3GPP TS 38.214 V16.6.0, Jun. 2021.
- [38] W. Wang, D. Cai, Z. Dong, L. Yu, Y. Xu, and Z. Liu, "Two-view image semantic cooperative non-orthogonal transmission in distributed edge networks," *Int. J. Intell. Syst.*, 2024.
- [39] H. Jin, K. Liu, M. Zhang, L. Zhang, G. Lee, E. N. Farag, D. Zhu, E. Onggosanusi, M. Shafi, and H. Tataria, "Massive MIMO evolution towards 3GPP release 18," *IEEE J. Sel. Areas Commun.*, 2023.
- [40] I. T. U. R. S. (ITU-R), "Framework and overall objectives of the future development of IMT for 2030 and beyond," Draft New Recommendation, 2023, available from the ITU-R, document under development.
- [41] J. Zhu, S. Liao, S. Li, and Q. Xue, "Additively manufactured metal-only millimeter-wave dual circularly polarized reflectarray antenna with independent control of polarizations," *IEEE Trans. Antennas Propag.*, vol. 70, no. 10, pp. 9918–9923, 2022.
- [42] P. Mahouti, M. A. Belen, N. Çalik, and S. Koziel, "Computationally efficient surrogate-assisted design of pyramidal-shaped 3-D reflectarray antennas," *IEEE Trans. Antennas Propag.*, vol. 70, no. 11, pp. 10777–10786, 2022.
- [43] R. Mali, R. Jatav, P. S. Rathore, R. Bharati, U. Singh, and M. K. Meshram, "Design of 1-bit high gain reflectarray antenna using dual reradiating element," in *2023 IEEE Microwaves, Antennas, Propag. Conf. IEEE*, 2023, pp. 1–4.
- [44] H. Q. Ngo, A. Ashikhmin, H. Yang, E. G. Larsson, and T. L. Marzetta, "Cell-free massive MIMO versus small cells," *IEEE Trans. Wireless Commun.*, vol. 16, no. 3, pp. 1834–1850, 2017.
- [45] A. Amiri, M. Angelichinoski, E. De Carvalho, and R. W. Heath, "Extremely large aperture massive MIMO: Low complexity receiver architectures," in *2018 IEEE GC Wkshps. IEEE*, 2018, pp. 1–6.
- [46] E. Björnson and L. Sanguinetti, "Power scaling laws and near-field behaviors of massive MIMO and intelligent reflecting surfaces," *IEEE Open J. Commun. Soc.*, vol. 1, pp. 1306–1324, 2020.
- [47] Y. Han, S. Jin, M. Matthaiou, T. Q. S. Quek, and C.-K. Wen, "Towards extra large-scale MIMO: New channel properties and low-cost designs," *IEEE Internet Things J.*, 2023.
- [48] H. Lu, Y. Zeng, C. You, Y. Han, J. Zhang, Z. Wang, Z. Dong, S. Jin, C.-X. Wang, T. Jiang *et al.*, "A tutorial on near-field XL-MIMO communications towards 6G," *IEEE Commun. Surv. Tutorials*, 2024.
- [49] N. B. Labs and AT&T, "Distributed massive MIMO," Available online at: <https://www.bell-labs.com/research-innovation/projects-and-initiatives/distributed-massive-mimo/>, accessed: 2022-02-28.
- [50] Huawei, "Huawei offers 5G distributed massive MIMO as the next evolution in indoor cellular networks," Available online at: <https://www.verdict.co.uk/huawei-offers-5g-massive-mimo-indoors/>, accessed: 2022-11-17.
- [51] X. Gao, F. Tufvesson, O. Edfors, and F. Rusek, "Measured propagation characteristics for very-large MIMO at 2.6 GHz," in *Asilomar Conference on Signals, Systems and Computers (ASILOMAR)*, 2012, pp. 295–299.
- [52] Z. Wang, J. Zhang, H. Du, D. Niyato, S. Cui, B. Ai, M. Debbah, K. B. Letaief, and H. V. Poor, "A tutorial on extremely large-scale MIMO for 6G: Fundamentals, signal processing, and applications," *IEEE Commun. Surv. Tutorials*, 2024.

- [53] G. Interdonato, E. Björnson, H. Quoc Ngo, P. Frenger, and E. G. Larsson, "Ubiquitous cell-free massive MIMO communications," *EURASIP J. Wireless Commun. Networking*, vol. 2019, no. 1, pp. 1–13, 2019.
- [54] S. Elhoushy, M. Ibrahim, and W. Hamouda, "Cell-free massive MIMO: A survey," *IEEE Commun. Surv. Tutorials*, vol. 24, no. 1, pp. 492–523, 2021.
- [55] C. Pan, G. Zhou, K. Zhi, S. Hong, T. Wu, Y. Pan, H. Ren, M. Di Renzo, A. L. Swindlehurst, R. Zhang *et al.*, "An overview of signal processing techniques for RIS/IRS-aided wireless systems," *IEEE J. Sel. Top. Signal Process.*, vol. 16, no. 5, pp. 883–917, 2022.
- [56] J. Zhang, E. Björnson, M. Matthaiou, D. W. K. Ng, H. Yang, and D. J. Love, "Prospective multiple antenna technologies for beyond 5G," *IEEE J. Sel. Areas Commun.*, vol. 38, no. 8, pp. 1637–1660, 2020.
- [57] E. Björnson, R. Zakhour, D. Gesbert, and B. Ottersten, "Cooperative multicell precoding: Rate region characterization and distributed strategies with instantaneous and statistical CSI," *IEEE Trans. Signal Process.*, vol. 58, no. 8, pp. 4298–4310, 2010.
- [58] R. Bhagavatula and R. W. Heath, "Adaptive limited feedback for sum-rate maximizing beamforming in cooperative multicell systems," *IEEE Trans. Signal Process.*, vol. 59, no. 2, pp. 800–811, 2011.
- [59] 3GPP, "Multi-connectivity stage 2 (release 17) TS 37.340 v17.7.0," *TSG RAN 2*, 2023.
- [60] C. Shepard, H. Yu, N. Anand, E. Li, T. Marzetta, R. Yang, and L. Zhong, "Argos: Practical many-antenna base stations," in *Proceedings of the 18th annual international conference on Mobile computing and networking*, 2012, pp. 53–64.
- [61] C. Shepard, H. Yu, and L. Zhong, "Argosv2: A flexible many-antenna research platform," in *Proceedings of the 19th annual international conference on Mobile computing and networking*, 2013, pp. 163–166.
- [62] J. Vieira, S. Malkowsky, K. Nieman, Z. Miers, N. Kundargi, L. Liu, I. Wong, V. owall, O. Edfors, and F. Tufvesson, "A flexible 100-antenna testbed for massive MIMO," in *2014 IEEE Globecom Workshops (GC Wkshps)*, 2014, pp. 287–293.
- [63] S. Malkowsky, J. Vieira, L. Liu, P. Harris, K. Nieman, N. Kundargi, I. C. Wong, F. Tufvesson, V. owall, and O. Edfors, "The world's first real-time testbed for massive MIMO: Design, implementation, and validation," *IEEE Access*, vol. 5, pp. 9073–9088, 2017.
- [64] Q. Yang, X. Li, H. Yao, J. Fang, K. Tan, W. Hu, J. Zhang, and Y. Zhang, "Bigstation: Enabling scalable real-time signal processing in large MU-MIMO systems," *ACM SIGCOMM Computer Communication Review*, vol. 43, no. 4, pp. 399–410, 2013.
- [65] K. Li, R. R. Sharan, Y. Chen, T. Goldstein, J. R. Cavallaro, and C. Studer, "Decentralized baseband processing for massive MU-MIMO systems," *IEEE J. Emerging Sel. Top. Circuits Syst.*, vol. 7, no. 4, pp. 491–507, Dec. 2017.
- [66] "Common public radio interface: ecpr interface specification," 2018.
- [67] A. Zaib, M. Masood, A. Ali, W. Xu, and T. Y. Al-Naffouri, "Distributed channel estimation and pilot contamination analysis for massive mimo-ofdm systems," *IEEE Trans. Commun.*, vol. 64, no. 11, pp. 4607–4621, 2016.
- [68] C. Zuo, H. Deng, J. Zhang, and Y. Qi, "Distributed channel estimation algorithm for mmwave massive MIMO communication systems," in *IEEE VTC-Fall*, 2021, pp. 1–6.
- [69] M. Trigka, C. Mavroukafalidis, and K. Berberidis, "A distributed sparse channel estimation technique for mmwave massive MIMO systems," in *29th EUSIPCO*, IEEE, 2021, pp. 2154–2158.
- [70] C. Tan, D. Cai, F. Fang, Z. Ding, and P. Fan, "Federated unfolding learning for CSI feedback in distributed edge networks," *IEEE Trans. Commun.*, 2024.
- [71] Y. Xu, B. Wang, E. Song, Q. Shi, and T.-H. Chang, "Low-complexity channel estimation for massive MIMO systems with decentralized baseband processing," *IEEE Trans. Signal Process.*, vol. 71, pp. 2728–2743, 2023.
- [72] T.-H. Chang, W.-C. Chiang, Y.-W. P. Hong, and C.-Y. Chi, "Training sequence design for discriminatory channel estimation in wireless MIMO systems," *IEEE Trans. Signal Process.*, vol. 58, no. 12, pp. 6223–6237, 2010.
- [73] Y. Takano, H.-J. Su, M. Juntti, and T. Matsumoto, "A conditional  $\ell_1$  regularized MMSE channel estimation technique for IBI channels," *IEEE Trans. Wireless Commun.*, vol. 17, no. 10, pp. 6720–6734, 2018.
- [74] C. Wei, H. Liu, Z. Zhang, J. Dang, and L. Wu, "Near-optimum sparse channel estimation based on least squares and approximate message passing," *IEEE Wireless Commun. Lett.*, vol. 6, no. 6, pp. 754–757, 2017.
- [75] X. Cheng, K. Xu, J. Sun, and S. Li, "Adaptive grouping sparse bayesian learning for channel estimation in non-stationary uplink massive MIMO systems," *IEEE Trans. Wireless Commun.*, vol. 18, no. 8, pp. 4184–4198, 2019.
- [76] N. Shariati, E. Björnson, M. Bengtsson, and M. Debbah, "Low-complexity polynomial channel estimation in large-scale MIMO with arbitrary statistics," *IEEE J. Sel. Top. Signal Process.*, vol. 8, no. 5, pp. 815–830, 2014.
- [77] C. Jeon, K. Li, J. R. Cavallaro, and C. Studer, "On the achievable rates of decentralized equalization in massive MU-MIMO systems," in *IEEE Int. Symp. Inf. Theory*, Jun. 2017, pp. 1102–1106.
- [78] Z. Zhang, H. Li, Y. Dong, X. Wang, and X. Dai, "Decentralized signal detection via expectation propagation algorithm for uplink massive MIMO systems," *IEEE Trans. Veh. Technol.*, vol. 69, no. 10, pp. 11 233–11 240, 2020.
- [79] Y. Dong, H. Li, C. Gong, X. Wang, and X. Dai, "An enhanced fully decentralized detector for the uplink M-MIMO system," *IEEE Trans. Veh. Technol.*, vol. 71, no. 12, pp. 13 030–13 042, 2022.
- [80] H. Li, Y. Dong, C. Gong, X. Wang, and X. Dai, "Gaussian message passing detection with constant front-haul signaling for cell-free massive MIMO," *IEEE Trans. Veh. Technol.*, vol. 72, no. 4, pp. 5395–5400, 2022.
- [81] Z. Zhang, Y. Dong, K. Long, X. Wang, and X. Dai, "Decentralized baseband processing with gaussian message passing detection for uplink massive MU-MIMO systems," *IEEE Trans. Veh. Technol.*, vol. 71, no. 2, pp. 2152–2157, Feb. 2022.
- [82] C. Jeon, K. Li, J. R. Cavallaro, and C. Studer, "Decentralized equalization with feedforward architectures for massive MU-MIMO," *IEEE Trans. Signal Process.*, vol. 67, no. 17, pp. 4418–4432, Sept. 2019.
- [83] V. Croisfelt, T. Abrao, A. Amiri, E. de Carvalho, and P. Popovski, "Decentralized design of fast iterative receivers for massive MIMO with spatial non-stationarities," in *55th Asilomar Conf. Signals, Syst., Comput.*, 2021, pp. 1242–1249.
- [84] A. Kulkarni, M. A. Ouameur, and D. Massicotte, "Hardware topologies for decentralized large-scale MIMO detection using newton method," *IEEE Trans. Circuits Syst. I Regul. Pap.*, vol. 68, no. 9, pp. 3732–3745, Sept. 2021.
- [85] J. Rodriguez Sanchez, F. Rusek, O. Edfors, and L. Liu, "Distributed and scalable uplink processing for LIS: Algorithm, architecture, and design trade-offs," *IEEE Trans. Signal Process.*, vol. 70, pp. 2639–2653, Apr. 2022.
- [86] A. Amiri, C. N. Manchón, and E. de Carvalho, "Uncoordinated and decentralized processing in extra-large MIMO arrays," *IEEE Wireless Commun. Lett.*, vol. 11, no. 1, pp. 81–85, Jan. 2022.
- [87] S.-H. Park, O. Simeone, O. Sahin, and S. Shamai, "Joint decompression and decoding for cloud radio access networks," *IEEE Signal Process. Lett.*, vol. 20, no. 5, pp. 503–506, 2013.
- [88] Y. Zhou and W. Yu, "Optimized backhaul compression for uplink cloud radio access network," *IEEE J. Sel. Areas Commun.*, vol. 32, no. 6, pp. 1295–1307, 2014.
- [89] S.-H. Park, O. Simeone, O. Sahin, and S. S. Shitz, "Fronthaul compression for cloud radio access networks: Signal processing advances inspired by network information theory," *IEEE Signal Process. Mag.*, vol. 31, no. 6, pp. 69–79, 2014.
- [90] B. Dai and W. Yu, "Energy efficiency of downlink transmission strategies for cloud radio access networks," *IEEE J. Sel. Areas Commun.*, vol. 34, no. 4, pp. 1037–1050, 2016.
- [91] Y. Zhou and W. Yu, "Fronthaul compression and transmit beamforming optimization for multi-antenna uplink C-RAN," *IEEE Trans. Signal Process.*, vol. 64, no. 16, pp. 4138–4151, 2016.
- [92] F. Wiffen, W. H. Chin, and A. Doufexi, "Distributed dimension reduction for distributed massive MIMO C-RAN with finite fronthaul capacity," in *55th Asilomar Conf. Signals, Syst., Comput.*, IEEE, 2021, pp. 1228–1236.
- [93] E. Song, Y. Zhu, and J. Zhou, "Sensors' optimal dimensionality compression matrix in estimation fusion," *Autom.*, vol. 41, no. 12, pp. 2131–2139, 2005.
- [94] I. D. Schizas, G. B. Giannakis, and Z.-Q. Luo, "Distributed estimation using reduced-dimensionality sensor observations," *IEEE Trans. Signal Process.*, vol. 55, no. 8, pp. 4284–4299, 2007.
- [95] L. Zhang, D. Niu, E. Song, J. Zhou, Q. Shi, and Y. Zhu, "Joint optimization of dimension assignment and compression in distributed estimation fusion," *IEEE Trans. Signal Process.*, vol. 67, no. 9, pp. 2453–2468, 2019.
- [96] L. Zhang, D. Niu, T. Ma, E. Song, Z. Li, and Q. Shi, "Joint dimension assignment and compression for deterministic parameter vector estimation in distributed multisensor networks," *IEEE Trans. Signal Process.*, vol. 69, pp. 2114–2128, 2021.

- [97] X. Zhao, M. Li, B. Wang, E. Song, T.-H. Chang, and Q. Shi, "Decentralized equalization for massive MIMO systems with colored noise samples," *arXiv preprint arXiv:2305.12805*, 2023.
- [98] Y. Xu, L. Zhu, R. Shi, and T.-H. Chang, "Joint compression and multiuser equalization for multi-carrier massive MIMO systems with decentralized baseband processing," *IEEE Trans. Signal Process.*, vol. 72, pp. 5708–5724, 2024.
- [99] M. Hong, Z.-Q. Luo, and M. Razaviyayn, "Convergence analysis of alternating direction method of multipliers for a family of nonconvex problems," *SIAM J. Optim.*, vol. 26, no. 1, pp. 337–364, 2016.
- [100] T.-H. Chang, M. Hong, and X. Wang, "Multi-agent distributed optimization via inexact consensus ADMM," *IEEE Trans. Signal Process.*, vol. 63, no. 2, pp. 482–497, 2014.
- [101] M. Sarajlic, F. Rusek, J. Rodríguez Sanchez, L. Liu, and O. Edfors, "Fully decentralized approximate zero-forcing precoding for massive MIMO systems," *IEEE Wireless Commun. Lett.*, vol. 8, no. 3, pp. 773–776, Jun. 2019.
- [102] J. V. Alegria, F. Rusek, and O. Edfors, "Trade-offs in decentralized multi-antenna architectures: The WAX decomposition," *IEEE Trans. Signal Process.*, vol. 69, pp. 3627–3641, Jun. 2021.
- [103] K. Li, C. Jeon, J. R. Cavallaro, and C. Studer, "Feedforward architectures for decentralized precoding in massive MU-MIMO systems," in *52nd Asilomar Conf. Signals, Syst., Comput.*, Oct. 2018, pp. 1659–1665.
- [104] J. Rodríguez Sanchez, F. Rusek, O. Edfors, M. Sarajlic, and L. Liu, "Decentralized massive MIMO processing exploring daisy-chain architecture and recursive algorithms," *IEEE Trans. Signal Process.*, vol. 68, pp. 687–700, Jan. 2020.
- [105] K. Li, J. McNaney, C. Tarver, O. Castañeda, C. Jeon, J. R. Cavallaro, and C. Studer, "Design trade-offs for decentralized baseband processing in massive MU-MIMO systems," in *53rd Asilomar Conf. Signals, Syst., Comput.*, Nov. 2019, pp. 906–912.
- [106] J. R. Sanchez, J. Vidal Alegria, and F. Rusek, "Decentralized massive MIMO systems: Is there anything to be discussed?" in *IEEE Int. Symp. Inf. Theory*, Jul. 2019, pp. 787–791.
- [107] X. Zhao, M. Li, Y. Liu, T.-H. Chang, and Q. Shi, "Communication-efficient decentralized linear precoding for massive MU-MIMO systems," *IEEE Trans. Signal Process.*, 2023.
- [108] Y. Zhou, Y. Xu, W. Yu, and J. Chen, "On the optimal fronthaul compression and decoding strategies for uplink cloud radio access networks," *IEEE Trans. Inf. Theory*, vol. 62, no. 12, pp. 7402–7418, 2016.
- [109] Y.-F. Liu, T.-H. Chang, M. Hong, Z. Wu, A. M.-C. So, E. A. Jorswieck, and W. Yu, "A survey of advances in optimization methods for wireless communication system design," *arXiv preprint arXiv:2401.12025*, 2024.
- [110] R. Shi, Y. Xu, L. Zhu, and T.-H. Chang, "Linear compression-based precoding for massive MIMO systems with decentralized baseband processing," *accepted by IEEE ICC*, 2024.
- [111] Q. Shi, M. Razaviyayn, Z.-Q. Luo, and C. He, "An iteratively weighted MMSE approach to distributed sum-utility maximization for a MIMO interfering broadcast channel," *IEEE Trans. Signal Process.*, vol. 59, no. 9, pp. 4331–4340, 2011.
- [112] L. Sun and M. R. McKay, "Eigen-based transceivers for the MIMO broadcast channel with semi-orthogonal user selection," *IEEE Trans. Signal Process.*, vol. 58, no. 10, pp. 5246–5261, 2010.
- [113] E. Björnson, J. Hoydis, and L. Sanguinetti, "Massive MIMO has unlimited capacity," *IEEE Trans. Wireless Commun.*, vol. 17, no. 1, pp. 574–590, Jan. 2018.
- [114] S. Wu, E. Björnson, C. Mollen, X. Tao, and E. G. Larsson, "Inverse extrapolation for efficient precoding in time-varying massive MIMO-OFDM systems," *IEEE Access*, vol. 7, pp. 91 105–91 119, Dec. 2019.
- [115] F. Kaltenberger, H. Jiang, M. Guillaud, and R. Knopp, "Relative channel reciprocity calibration in MIMO/TDD systems," in *Future Network and Mobile Summit*. IEEE, 2010, pp. 1–10.
- [116] J. Vieira, F. Rusek, O. Edfors, S. Malkowsky, L. Liu, and F. Tufvesson, "Reciprocity calibration for massive MIMO: Proposal, modeling, and validation," *IEEE Trans. Wireless Commun.*, vol. 16, no. 5, pp. 3042–3056, 2017.
- [117] P. Zetterberg, "Experimental investigation of TDD reciprocity-based zero-forcing transmit precoding," *EURASIP J. Adv. Signal Process.*, vol. 2011, pp. 1–10, 2011.
- [118] L. Chen, R. Nie, Y. Chen, and W. Wang, "Hierarchical-absolute reciprocity calibration for millimeter-wave hybrid beamforming systems," *IEEE Trans. Wireless Commun.*, 2022.
- [119] B. M. Lee, "Calibration for channel reciprocity in industrial massive MIMO antenna systems," *IEEE Trans. Ind. Inf.*, vol. 14, no. 1, pp. 221–230, 2017.
- [120] X. Jiang, M. Cirkic, F. Kaltenberger, E. G. Larsson, L. Deneire, and R. Knopp, "MIMO-TDD reciprocity under hardware imbalances: Experimental results," in *IEEE ICC*, 2015, pp. 4949–4953.
- [121] X. Luo, F. Yang, and H. Zhu, "Massive MIMO self-calibration: Optimal interconnection for full calibration," *IEEE Trans. Veh. Technol.*, vol. 68, no. 11, pp. 10 357–10 371, 2019.
- [122] H. Papadopoulos, O. Y. Bursalioglu, and G. Caire, "Avalanche: Fast RF calibration of massive arrays," in *IEEE GlobalSIP*, 2014.
- [123] X. Jiang, A. Decurninge, K. Gopala, F. Kaltenberger, M. Guillaud, D. Slock, and L. Deneire, "A framework for over-the-air reciprocity calibration for TDD massive MIMO systems," *IEEE Trans. Wireless Commun.*, vol. 17, no. 9, pp. 5975–5990, 2018.
- [124] R. Rogalin, O. Y. Bursalioglu, H. Papadopoulos, G. Caire, A. F. Molisch, A. Michaloliakos, V. Balan, and K. Psounis, "Scalable synchronization and reciprocity calibration for distributed multiuser MIMO," *IEEE Trans. Wireless Commun.*, vol. 13, no. 4, pp. 1815–1831, 2014.
- [125] J. Vieira and E. G. Larsson, "Reciprocity calibration of distributed massive MIMO access points for coherent operation," in *IEEE PIMRC*, 2021.
- [126] C.-M. Chen, S. Blandino, A. Gaber, C. Desset, A. Bourdoux, L. Van der Perre, and S. Pollin, "Distributed massive MIMO: A diversity combining method for TDD reciprocity calibration," in *Proc. IEEE GLOBE-COM*, 2017.
- [127] N.-I. Kim, C. W. Yu, S.-E. Hong, J.-H. Na, and B. C. Chung, "A gradual method for channel non-reciprocity calibration in cell-free massive MIMO," *IEEE Commun. Lett.*, vol. 26, no. 11, pp. 2779–2783, 2022.
- [128] Y. Cao, P. Wang, K. Zheng, X. Liang, D. Liu, M. Lou, J. Jin, Q. Wang, D. Wang, Y. Huang *et al.*, "Experimental performance evaluation of cell-free massive MIMO systems using COTS RRU with OTA reciprocity calibration and phase synchronization," *IEEE J. Sel. Areas Commun.*, pp. 1620–1634, 2023.
- [129] H. V. Balan, R. Rogalin, A. Michaloliakos, K. Psounis, and G. Caire, "AirSync: Enabling distributed multiuser MIMO with full spatial multiplexing," *IEEE/ACM Trans. Networking*, vol. 21, no. 6, pp. 1681–1695, 2013.
- [130] M. Rashid and J. A. Nanzer, "Frequency and phase synchronization in distributed antenna arrays based on consensus averaging and kalman filtering," *IEEE Trans. Wireless Commun.*, pp. 2789–2803, 2023.
- [131] U. K. Ganesan, R. Sarvendranath, and E. G. Larsson, "BeamSync: Over-the-air synchronization for distributed massive MIMO systems," *IEEE Trans. Wireless Commun.*, 2023.
- [132] E. G. Larsson, "Massive synchrony in distributed antenna systems," *IEEE Trans. Signal Process.*, 2024.
- [133] R. Nissel, "Correctly modeling TX and RX chain in (distributed) massive MIMO – new fundamental insights on coherency," *IEEE Commun. Lett.*, pp. 2465–2469, Oct. 2022.
- [134] E. G. Larsson and J. Vieira, "Phase calibration of distributed antenna arrays," *IEEE Commun. Lett.*, 2023.
- [135] A. Tolli, H. Pennanen, and P. Komulainen, "Decentralized minimum power multi-cell beamforming with limited backhaul signaling," *IEEE Trans. Wireless Commun.*, vol. 10, no. 2, pp. 570–580, 2011.
- [136] R. P. Antonioni, G. Fodor, P. Soldati, and T. F. Maciel, "Decentralized user scheduling for rate-constrained sum-utility maximization in the MIMO IBC," *IEEE Trans. Commun.*, vol. 68, no. 10, pp. 6215–6229, 2020.
- [137] T. Cai, S. Ge, Y. Xu, and T.-H. Chang, "Approaching centralized multi-cell coordinated beamforming with limited backhaul signaling," in *ICC 2023 - IEEE International Conference on Communications*, 2023, pp. 3559–3564.
- [138] D. Gesbert, S. Hanly, H. Huang, S. S. Shitz, O. Simeone, and W. Yu, "Multi-cell MIMO cooperative networks: A new look at interference," *IEEE J. Sel. Areas Commun.*, vol. 28, no. 9, pp. 1380–1408, 2010.
- [139] M. Hong, R. Sun, H. Baligh, and Z.-Q. Luo, "Joint base station clustering and beamformer design for partial coordinated transmission in heterogeneous networks," *IEEE J. Sel. Areas Commun.*, vol. 31, no. 2, pp. 226–240, 2013.
- [140] G. Nigam, P. Minero, and M. Haenggi, "Coordinated multipoint joint transmission in heterogeneous networks," *IEEE Trans. Commun.*, vol. 62, no. 11, pp. 4134–4146, 2014.
- [141] J. Park, N. Lee, and R. W. Heath, "Cooperative base station coloring for pair-wise multi-cell coordination," *IEEE Trans. Commun.*, vol. 64, no. 1, pp. 402–415, 2015.



- [142] C. Shen, T.-H. Chang, K.-Y. Wang, Z. Qiu, and C.-Y. Chi, "Distributed robust multicell coordinated beamforming with imperfect CSI: An ADMM approach," *IEEE Trans. Signal Process.*, vol. 60, no. 6, pp. 2988–3003, 2012.
- [143] M. Maros and J. Jalden, "ADMM for distributed dynamic beamforming," *IEEE Trans. Signal Inf. Process. Networks*, vol. 4, no. 2, pp. 220–235, 2018.
- [144] I. Boukhedimi, A. Kammoun, and M.-S. Alouini, "Coordinated slnr based precoding in large-scale heterogeneous networks," *IEEE J. Sel. Top. Signal Process.*, vol. 11, no. 3, pp. 534–548, 2017.
- [145] Z. Li, T. Gamvrelis, H. A. Ammar, and R. Adve, "Decentralized user scheduling and beamforming in multi-cell MIMO networks," in *IEEE Int. Conf. Commun.* IEEE, 2022, pp. 1980–1985.
- [146] D. Han and N. Lee, "Distributed precoding using local CSIT for MU-MIMO heterogeneous cellular networks," *IEEE Trans. Commun.*, vol. 69, no. 3, pp. 1666–1678, 2020.
- [147] H. Pennanen, A. Tolli, and M. Latva-aho, "Decentralized coordinated downlink beamforming via primal decomposition," *IEEE Signal Process. Lett.*, vol. 18, no. 11, pp. 647–650, 2011.
- [148] I. Atzeni, B. Gouda, and A. Tolli, "Distributed precoding design via over-the-air signaling for cell-free massive MIMO," *IEEE Trans. Wireless Commun.*, vol. 20, no. 2, pp. 1201–1216, 2020.
- [149] A. A. Khan, R. Adve, and W. Yu, "Optimizing multicell scheduling and beamforming via fractional programming and hungarian algorithm," in *2018 IEEE Globecom Workshops (GC Wkshps)*. IEEE, 2018, pp. 1–6.
- [150] D. W. K. Ng and R. Schober, "Resource allocation and scheduling in multi-cell OFDMA systems with decode-and-forward relaying," *IEEE Trans. Wireless Commun.*, vol. 10, no. 7, pp. 2246–2258, 2011.
- [151] T. Cai, L. Li, and T.-H. Chang, "Sensing-assisted distributed user scheduling and beamforming in multi-cell mmWave networks," in *IEEE ICASSP*, 2024, pp. 81–85.
- [152] O. T. Demir, M. Masoudi, E. Björnson, and C. Cavdar, "Cell-free massive MIMO in O-RAN: Energy-aware joint orchestration of cloud, fronthaul, and radio resources," *IEEE J. Sel. Areas Commun.*, 2024.
- [153] M. H. Lee, C. Yun, G. H. Kim, S. Y. Park, C. W. Yu, and K. W. Choi, "Fully distributed cell-free MIMO systems: Architecture, algorithm, and testbed experiments," *IEEE Internet Things J.*, vol. 11, no. 5, pp. 7956–7973, 2024.
- [154] E. Björnson and L. Sanguinetti, "Making cell-free massive MIMO competitive with MMSE processing and centralized implementation," *IEEE Trans. Wireless Commun.*, vol. 19, no. 1, pp. 77–90, 2020.
- [155] G. Interdonato, M. Karlsson, E. Björnson, and E. G. Larsson, "Local partial zero-forcing precoding for cell-free massive MIMO," *IEEE Trans. Wireless Commun.*, vol. 19, no. 7, pp. 4758–4774, 2020.
- [156] I. Atzeni, B. Gouda, and A. Tolli, "Distributed precoding design via over-the-air signaling for cell-free massive MIMO," *IEEE Trans. Wireless Commun.*, vol. 20, no. 2, pp. 1201–1216, 2021.
- [157] E. Björnson and L. Sanguinetti, "Scalable cell-free massive MIMO systems," *IEEE Trans. Commun.*, vol. 68, no. 7, pp. 4247–4261, 2020.
- [158] C. D'Andrea and E. G. Larsson, "User association in scalable cell-free massive MIMO systems," in *2020 54th Asilomar Conference on Signals, Systems, and Computers*. IEEE, 2020, pp. 826–830.
- [159] Z. H. Shaik, E. Björnson, and E. G. Larsson, "MMSE-optimal sequential processing for cell-free massive MIMO with radio stripes," *IEEE Trans. Commun.*, vol. 69, no. 11, pp. 7775–7789, 2021.
- [160] L. Miretti, E. Björnson, and D. Gesbert, "Team MMSE precoding with applications to cell-free massive MIMO," *IEEE Trans. Wireless Commun.*, vol. 21, no. 8, pp. 6242–6255, 2022.
- [161] O. T. Demir, E. Björnson, L. Sanguinetti *et al.*, "Foundations of user-centric cell-free massive MIMO," *Found. Trend. Signal Process.*, vol. 14, no. 3–4, pp. 162–472, 2021.
- [162] H. A. Ammar, R. Adve, S. Shahbazpanahi, G. Boudreau, and K. V. Srinivas, "Distributed resource allocation optimization for user-centric cell-free MIMO networks," *IEEE Trans. Wireless Commun.*, vol. 21, no. 5, pp. 3099–3115, 2022.
- [163] Z. Li, F. Gottsch, S. Li, M. Chen, and G. Caire, "Joint fronthaul load balancing and computation resource allocation in cell-free user-centric massive MIMO networks," *IEEE Trans. Wireless Commun.*, pp. 1–1, 2024.
- [164] E. Jorswieck, "Next generation multiple access: From basic principles to modern architectures," *Proc. of IEEE*, 2024.
- [165] S. Elhoushy, M. Ibrahim, and W. Hamouda, "Cell-free massive MIMO: A survey," *IEEE Commun. Surv. Tutorials*, vol. 24, no. 1, pp. 492–523, 2022.
- [166] L. Diez, A. M. Alba, W. Kellerer, and R. Aguero, "Flexible functional split and fronthaul delay: A queuing-based model," *IEEE Access*, vol. 9, pp. 151 049–151 066, 2021.
- [167] E. Jorswieck, L. Kunz, R. Raghunath, and B. Peng, "Rate-splitting downlink transmission in cell-free networks under fronthaul constraints," in *Proc. IEEE ISWCS*, 2024.
- [168] Y. Fang, L. Qiu, X. Liang, and C. Ren, "Cell-free massive MIMO systems with oscillator phase noise: Performance analysis and power control," *IEEE Trans. Veh. Technol.*, vol. 70, no. 10, pp. 10048–10064, 2021.
- [169] K. Ando, H. Iimori, T. Takahashi, K. Ishibashi, and G. T. F. De Abreu, "Uplink signal detection for scalable cell-free massive MIMO systems with robustness to rate-limited fronthaul," *IEEE Access*, vol. 9, pp. 102 770–102 782, 2021.
- [170] M. Cui, Z. Wu, Y. Lu, X. Wei, and L. Dai, "Near-field MIMO communications for 6G: Fundamentals, challenges, potentials, and future directions," *IEEE Commun. Mag.*, vol. 61, no. 1, pp. 40–46, 2023.
- [171] Q. Wu and R. Zhang, "Reconfigurable intelligent surfaces: Principles and opportunities," *arXiv preprint arXiv:2007.03435*, 2020.
- [172] M. Jian, G. C. Alexandropoulos, E. Basar, C. Huang, R. Liu, Y. Liu, and C. Yuen, "Reconfigurable intelligent surfaces for wireless communications: Overview of hardware designs, channel models, and estimation techniques," *arXiv preprint arXiv:2203.03176*, 2022.
- [173] S. Willhammar, H. Iimori, J. Vieira, L. Sundstrom, F. Tufvesson, and E. G. Larsson, "Achieving distributed MIMO performance with repeater-assisted cellular massive MIMO," 2024, to appear in the *IEEE Commun. Mag.*
- [174] E. G. Larsson and J. Vieira, and P. Frenger, "Reciprocity calibration of dual-antenna repeaters," *IEEE Wireless Commun. Lett.*, vol. 13, no. 6, pp. 1606–1610, 2024.
- [175] E. G. Larsson and J. Bai, "Stability analysis of interacting wireless repeaters," in *to appear in Proc. of IEEE SPAWC*, 2024.
- [176] L. Liu, R. Zhang, and K.-C. Chua, "Multi-antenna wireless powered communication with energy beamforming," *IEEE Trans. Commun.*, vol. 62, no. 12, pp. 4349–4361, Dec. 2014.
- [177] D. Mishra and E. G. Larsson, "Optimal channel estimation for reciprocity-based backscattering with a full-duplex MIMO reader," *IEEE Trans. Signal Process.*, vol. 67, no. 6, pp. 1662–1677, Mar. 2019.
- [178] S. Kashyap, E. Björnson, and E. G. Larsson, "On the feasibility of wireless energy transfer using massive antenna arrays," *IEEE Trans. Wireless Commun.*, vol. 15, pp. 3466–3480, May 2016.
- [179] J. Kimionis, A. Bletsas, and J. N. Sahalos, "Increased range bistatic scatter radio," *IEEE Trans. Commun.*, vol. 62, pp. 1091–1104, Mar. 2014.
- [180] M. Hua, L. Yang, C. Li, Z. Zhu, and I. Lee, "Bistatic backscatter communication: Shunt network design," *IEEE Internet Things J.*, vol. 8, no. 9, pp. 7691–7705, Nov. 2020.
- [181] S. Basharat, S. A. Hassan, A. Mahmood, Z. Ding, and M. Gidlund, "Reconfigurable intelligent surface-assisted backscatter communication: A new frontier for enabling 6G IoT networks," *arXiv preprint arXiv:2107.07813*, 2021.
- [182] R. Biswas, M. U. Sheikh, H. Yigitler, J. Lempiainen, and R. Jantti, "Direct path interference suppression requirements for bistatic backscatter communication system," in *Proc. IEEE VTC-Spring*, Apr. 2021.
- [183] A. Varshney, O. Harms, C. Perez-Penichet, C. Rohner, F. Hermans, and T. Voigt, "Lorea: A backscatter architecture that achieves a long communication range," in *Proc. ACM Conf. Embedded Netw. Sensor Syst.*, Nov. 2017.
- [184] D. Li, "Capacity of backscatter communication with frequency shift in Rician fading channels," *IEEE Wireless Commun. Lett.*, vol. 8, no. 6, pp. 1639–1643, Dec. 2019.
- [185] A. Kaplan, J. Vieira, and E. G. Larsson, "Direct link interference suppression for bistatic backscatter communication in distributed MIMO," *IEEE Trans. Wireless Commun.*, 2023.
- [186] Q. Tao, Y. Li, C. Zhong, S. Shao, and Z. Zhang, "A novel interference cancellation scheme for bistatic backscatter communication systems," *IEEE Commun. Lett.*, vol. 25, no. 6, pp. 2014–2018, Jun. 2021.
- [187] B. J. B. Deutschmann, T. Wilding, E. G. Larsson, and K. Witrisal, "Location-based initial access for wireless power transfer with physically large arrays," *IEEE ICC*, 2022.
- [188] S. S. Thoota, J. Vieira, and E. G. Larsson, "Data-driven robust beamforming for initial access," *IEEE Globecom 2023. arXiv preprint arXiv:2308.07132*.
- [189] A. Kaplan, D. M. Osorio, and E. G. Larsson, "Access point selection for bistatic backscatter communication in cell-free MIMO," in *Proc. IEEE ICC*, 2024.
- [190] D. Dardari, "Communicating with large intelligent surfaces: Fundamental limits and models," *IEEE J. Sel. Areas Commun.*, vol. 38, no. 11, pp. 2526–2537, 2020.

- [191] K. Zhi, C. Pan, G. Zhou, H. Ren, M. El Kashlan, and R. Schober, "Is RIS-aided massive MIMO promising with ZF detectors and imperfect CSI?" *IEEE J. Sel. Areas Commun.*, vol. 40, no. 10, pp. 3010–3026, 2022.
- [192] J. Sang, Y. Yuan, W. Tang, Y. Li, X. Li, S. Jin, Q. Cheng, and T. J. Cui, "Coverage enhancement by deploying RIS in 5G commercial mobile networks: Field trials," *IEEE Wireless Commun.*, vol. 31, no. 1, pp. 172–180, 2024.
- [193] J. Sang, M. Zhou, J. Lan, B. Gao, W. Tang, X. Li, S. Jin, C. Li, Q. Cheng, and T. J. Cui, "Multi-scenario broadband channel measurement and modeling for sub-6 GHz RIS-assisted wireless communication systems," *IEEE Trans. Wireless Commun.*, vol. 23, no. 6, pp. 6312–6329, 2024.
- [194] X. Li, L. Jiang, C. Luo, Y. Han, M. Matthaiou, and S. Jin, "RIS-enhanced multi-cell downlink transmission using statistical channel state information," *Sci. China Inf. Sci.*, vol. 66, no. 11, p. 212301, 2023.
- [195] L. Jiang, X. Li, M. Matthaiou, and S. Jin, "Joint user scheduling and phase shift design for RIS assisted multi-cell MISO systems," *IEEE Wireless Commun. Lett.*, vol. 12, no. 3, pp. 431–435, 2022.
- [196] J. Sang, J. Lan, M. Zhou, B. Gao, W. Tang, X. Li, X. Yi, and S. Jin, "Quantized phase alignment by discrete phase shifts for reconfigurable intelligent surface-assisted communication systems," *IEEE Trans. Veh. Technol.*, vol. 73, no. 4, pp. 5259–5275, 2024.
- [197] P. Chen, X. Li, M. Matthaiou, and S. Jin, "DRL-based RIS phase shift design for OFDM communication systems," *IEEE Wireless Commun. Lett.*, vol. 12, no. 4, pp. 733–737, 2023.
- [198] H. Li, S. Shen, and B. Clerckx, "Beyond diagonal reconfigurable intelligent surfaces: From transmitting and reflecting modes to single-, group-, and fully-connected architectures," *IEEE Trans. Wireless Commun.*, vol. 22, no. 4, pp. 2311–2324, 2023.
- [199] I. Santamaria, M. Soleymani, E. Jorswieck, and J. Gutierrez, "Snr maximization in beyond diagonal ris-assisted single and multiple antenna links," *IEEE Signal Process. Lett.*, vol. 30, pp. 923–926, 2023.
- [200] M. Soleymani, I. Santamaria, and E. A. Jorswieck, "Rate splitting in MIMO RIS-assisted systems with hardware impairments and improper signaling," *IEEE Trans. Veh. Technol.*, vol. 72, no. 4, pp. 4580–4597, 2022.
- [201] M. Soleymani, I. Santamaria, E. Jorswieck, and S. Rezvani, "NOMA-based improper signaling for multicell MISO RIS-assisted broadcast channels," *IEEE Trans. Signal Process.*, vol. 71, pp. 963–978, 2023.
- [202] M. Soleymani, I. Santamaria, E. Jorswieck, and B. Clerckx, "Optimization of rate-splitting multiple access in beyond diagonal RIS-assisted URLLC systems," *IEEE Trans. Wireless Commun.*, 2023.
- [203] M. Soleymani, I. Santamaria, and E. Jorswieck, "Spectral and energy efficiency maximization of MISO STAR-RIS-assisted URLLC systems," *IEEE Access*, 2023.
- [204] T. Van Chien, H. Q. Ngo, S. Chatzinotas, M. Di Renzo, and B. Ottersten, "Reconfigurable intelligent surface-assisted cell-free massive MIMO systems over spatially-correlated channels," *IEEE Trans. Wireless Commun.*, vol. 21, no. 7, pp. 5106–5128, 2022.
- [205] X. Pei, H. Yin, L. Tan, L. Cao, Z. Li, K. Wang, K. Zhang, and E. Björnson, "RIS-aided wireless communications: Prototyping, adaptive beamforming, and indoor/outdoor field trials," *IEEE Trans. Commun.*, vol. 69, no. 12, pp. 8627–8640, 2021.
- [206] F. Liu, Y. Cui, C. Masouros, J. Xu, T. X. Han, Y. C. Eldar, and S. Buzzi, "Integrated sensing and communications: Toward dual-functional wireless networks for 6G and beyond," *IEEE J. Sel. Areas Commun.*, vol. 40, no. 6, pp. 1728–1767, Mar. 2022.
- [207] K. Zhang, Y. Xu, R. He, C. Shen, and T.-H. Chang, "Optimal joint fronthaul compression and beamforming design for networked ISAC systems," *arXiv preprint arXiv:2408.08057*, 2024.
- [208] E. C. Strinati, G. C. Alexandropoulos, N. Amani, M. Crozzoli, G. Madhusudan, S. Mekki, F. Rivet, V. Sciancalepore, P. Sehier, M. Stark *et al.*, "Towards distributed and intelligent integrated sensing and communications for 6G networks," *arXiv preprint arXiv:2402.11630*, 2024.
- [209] H. Guo, H. Wymeersch, B. Makki, H. Chen, Y. Wu, G. Durisi, M. F. Keskin, M. H. Moghaddam, C. Madapatha, H. Yu *et al.*, "Integrated communication, localization, and sensing in 6G D-MIMO networks," *arXiv preprint arXiv:2403.19785*, 2024.
- [210] J. Yang, C.-K. Wen, J. Xu, H. Que, H. Wei, and S. Jin, "Angle-based SLAM on 5G mmWave systems: Design, implementation, and measurement," *IEEE Internet Things J.*, vol. 10, no. 20, pp. 17755–17771, May 2023.
- [211] H. Que, J. Yang, C.-K. Wen, S. Xia, X. Li, and S. Jin, "Joint beam management and SLAM for mmwave communication systems," *IEEE Trans. Commun.*, vol. 71, no. 10, pp. 6162–6179, 2023.
- [212] J. Yang, C.-K. Wen, S. Jin, and X. Li, "Enabling plug-and-play and crowdsourcing SLAM in wireless communication systems," *IEEE Trans. Wireless Commun.*, vol. 21, no. 3, pp. 1453–1468, Mar. 2022.
- [213] H. Kim, K. Granstrom, L. Gao, G. Battistelli, S. Kim, and H. Wymeersch, "5GmmWave cooperative positioning and mapping using multi-model PHD filter and map fusion," *IEEE Trans. Wireless Commun.*, vol. 19, no. 6, pp. 3782–3795, Mar. 2020.
- [214] T. Du, J. Yang, S. Xia, and S. Jin, "Multi-BS fusion scheme for PHD simultaneous localization and mapping," in *Proc. ICCT*, 2023, pp. 439–444.
- [215] C. Tan, D. Cai, Y. Xu, Z. Ding, and P. Fan, "Threshold-enhanced hierarchical spatial non-stationary channel estimation for uplink massive MIMO systems," *IEEE Trans. Wireless Commun.*, vol. 23, no. 5, pp. 4830–4844, 2024.
- [216] M. Cui and L. Dai, "Channel estimation for extremely large-scale MIMO: Far-field or near-field?" *IEEE Trans. Commun.*, vol. 70, no. 4, pp. 2663–2677, 2022.
- [217] Y. Han, S. Jin, C.-K. Wen, and X. Ma, "Channel estimation for extremely large-scale massive MIMO systems," *IEEE Wireless Commun. Lett.*, vol. 9, no. 5, pp. 633–637, 2020.
- [218] H. Zhang, N. Shlezinger, F. Guidi, D. Dardari, M. F. Imani, and Y. C. Eldar, "Beam focusing for near-field multiuser MIMO communications," *IEEE Trans. Wireless Commun.*, vol. 21, no. 9, pp. 7476–7490, 2022.
- [219] Z. Ding, R. Schober, and H. V. Poor, "NOMA-based coexistence of near-field and far-field massive MIMO communications," *IEEE Wireless Commun. Lett.*, vol. 12, no. 8, pp. 1429–1433, 2023.
- [220] Z. Ding, "Resolution of near-field beamforming and its impact on NOMA," *IEEE Wireless Commun. Lett.*, vol. 13, no. 2, pp. 456–460, 2024.
- [221] K.-K. Wong, K.-F. Tong, Y. Shen, Y. Chen, and Y. Zhang, "Bruce lee-inspired fluid antenna system: Six research topics and the potentials for 6G," *Front. Commun. Networks*, vol. 3, p. 853416, 2022.
- [222] L. Zhu, W. Ma, and R. Zhang, "Movable antennas for wireless communication: Opportunities and challenges," *IEEE Commun. Mag.*, 2023.
- [223] K.-K. Wong, A. Shojaeifard, K.-F. Tong, and Y. Zhang, "Fluid antenna systems," *IEEE Trans. Wireless Commun.*, vol. 20, no. 3, pp. 1950–1962, 2020.
- [224] L. Zhu, W. Ma, and R. Zhang, "Modeling and performance analysis for movable antenna enabled wireless communications," *IEEE Trans. Wireless Commun.*, 2023.
- [225] W. Ma, L. Zhu, and R. Zhang, "MIMO capacity characterization for movable antenna systems," *IEEE Trans. Wireless Commun.*, 2023.
- [226] K. K. Wong, A. Shojaeifard, K.-F. Tong, and Y. Zhang, "Performance limits of fluid antenna systems," *IEEE Commun. Lett.*, vol. 24, no. 11, pp. 2469–2472, 2020.
- [227] X. Shao and R. Zhang, "6DMA enhanced wireless network with flexible antenna position and rotation: Opportunities and challenges," *arXiv preprint arXiv:2406.06064*, 2024.
- [228] H. O. Y. Suzuki and K. Kawai, "Pinching antenna: Using a dielectric waveguide as an antenna," *NTT DOCOMO Technical J.*, Jan. 2022.
- [229] Z. Ding, R. Schober, and H. V. Poor, "Flexible-antenna systems: A pinching-antenna perspective," *arXiv preprint arXiv:2412.02376*, 2024.
- [230] L. Mucchi, S. Jayousi, S. Caputo, E. Panayirci, S. Shahabuddin, J. Bechtold, I. Morales, R.-A. Stoica, G. Abreu, and H. Haas, "Physical-layer security in 6G networks," *IEEE Open J. Commun. Soc.*, vol. 2, pp. 1901–1914, 2021.
- [231] A. Mukherjee, V. Kumar, E. Jorswieck, B. Ottersten, and L.-N. Tran, "On the optimality of the stationary solution of secrecy rate maximization for MIMO wiretap channel," *IEEE Wireless Commun. Lett.*, vol. 11, no. 2, pp. 357–361, 2022.
- [232] J. Choi and J. Park, "Sum secrecy spectral efficiency maximization in downlink MU-MIMO: Colluding eavesdroppers," *IEEE Trans. Veh. Technol.*, vol. 70, no. 1, pp. 1051–1056, 2021.
- [233] D. A. Tubail, M. Alsmadi, and S. Ikki, "Physical layer security in downlink of cell-free massive MIMO with imperfect CSI," *IEEE Trans. Inf. Forensics Secur.*, vol. 18, pp. 2945–2960, 2023.
- [234] J. Ferreira, J. Guerreiro, and R. Dinis, "Physical layer security with near-field beamforming," *IEEE Access*, vol. 12, pp. 4801–4811, 2024.
- [235] G. Li, Y. Xu, W. Xu, E. Jorswieck, and A. Hu, "Robust key generation with hardware mismatch for secure MIMO communications," *IEEE Trans. Inf. Forensics Secur.*, vol. 16, pp. 5264–5278, 2021.

- [236] G. Li, C. Sun, E. A. Jorswieck, J. Zhang, A. Hu, and Y. Chen, "Sum secret key rate maximization for TDD multi-user massive MIMO wireless networks," *IEEE Trans. Inf. Forensics Secur.*, vol. 16, pp. 968–982, 2021.
- [237] N. Xie, Z. Li, and H. Tan, "A survey of physical-layer authentication in wireless communications," *IEEE Commun. Surv. Tutorials*, vol. 23, no. 1, pp. 282–310, 2021.
- [238] S. J. Maeng, Y. Yapici, I. Guvenc, A. Bhuyan, and H. Dai, "Precoder design for physical-layer security and authentication in massive MIMO UAV communications," *IEEE Trans. Veh. Technol.*, vol. 71, no. 3, pp. 2949–2964, 2022.
- [239] J. Qiu, K. Xu, X. Xia, Z. Shen, W. Xie, D. Zhang, and M. Wang, "Secure transmission scheme based on fingerprint positioning in cell-free massive MIMO systems," *IEEE Trans. Signal Inf. Process. Networks*, vol. 8, pp. 92–105, 2022.
- [240] S. Jacobsson, G. Durisi, M. Coldrey, U. Gustavsson, and C. Studer, "One-bit massive MIMO: Channel estimation and high-order modulations," in *IEEE ICC Workshop*. IEEE, 2015, pp. 1304–1309.
- [241] —, "Throughput analysis of massive MIMO uplink with low-resolution ADCs," *IEEE Trans. Wireless Commun.*, vol. 16, no. 6, pp. 4038–4051, 2017.
- [242] Z. Wang, M. Li, Q. Liu, and A. L. Swindlehurst, "Hybrid precoder and combiner design with low-resolution phase shifters in mmwave MIMO systems," *IEEE J. Sel. Top. Signal Process.*, vol. 12, no. 2, pp. 256–269, 2018.
- [243] Y. Li, C. Tao, G. Seco-Granados, A. Mezghani, A. L. Swindlehurst, and L. Liu, "Channel estimation and performance analysis of one-bit massive MIMO systems," *IEEE Trans. Signal Process.*, vol. 65, no. 15, pp. 4075–4089, 2017.
- [244] M. Shao, W.-K. Ma, Q. Li, and A. L. Swindlehurst, "One-bit sigma-delta MIMO precoding," *IEEE J. Sel. Top. Signal Process.*, vol. 13, no. 5, pp. 1046–1061, 2019.
- [245] B. Fesl, N. Turan, B. Böck, and W. Utschick, "Channel estimation for quantized systems based on conditionally gaussian latent models," *IEEE Trans. Signal Process.*, 2024.
- [246] I. Atzeni and A. Tölli, "Channel estimation and data detection analysis of massive MIMO with 1-bit ADCs," *IEEE Trans. Wireless Commun.*, vol. 21, no. 6, pp. 3850–3867, 2021.
- [247] F. Sohrabi, Y.-F. Liu, and W. Yu, "One-bit precoding and constellation range design for massive MIMO with QAM signaling," *IEEE J. Sel. Top. Signal Process.*, vol. 12, no. 3, pp. 557–570, 2018.
- [248] M. Shao, Q. Li, W.-K. Ma, and A. M.-C. So, "A framework for one-bit and constant-envelope precoding over multiuser massive MISO channels," *IEEE Trans. Signal Process.*, vol. 67, no. 20, pp. 5309–5324, 2019.
- [249] C. Risi, D. Persson, and E. G. Larsson, "Massive MIMO with 1-bit ADC," *arXiv preprint arXiv:1404.7736*, 2014.
- [250] C. Studer and G. Durisi, "Quantized massive MU-MIMO-OFDM uplink," *IEEE Trans. Commun.*, vol. 64, no. 6, pp. 2387–2399, 2016.
- [251] M. Shao and W.-K. Ma, "Binary MIMO detection via homotopy optimization and its deep adaptation," *IEEE Trans. Signal Process.*, vol. 69, pp. 781–796, 2020.
- [252] C.-K. Wen, C.-J. Wang, S. Jin, K.-K. Wong, and P. Ting, "Bayes-optimal joint channel-and-data estimation for massive MIMO with low-precision ADCs," *IEEE Trans. Signal Process.*, vol. 64, no. 10, pp. 2541–2556, 2015.
- [253] S. Chen, S. Sun, and S. Kang, "System integration of terrestrial mobile communication and satellite communication—the trends, challenges and key technologies in B5G and 6G," *China commun.*, vol. 17, no. 12, pp. 156–171, 2020.
- [254] Y. He, C. Wang, C. Qi, and Z. Feng, "Spatial ultra-sparse distributed antenna satellite-ground cooperative transmission architecture: Challenges, key technologies, and trends," *IEEE Commun. Mag.*, 2024.
- [255] M. Y. Abdelsadek, G. K. Kurt, and H. Yanikomeroglu, "Distributed massive MIMO for LEO satellite networks," *IEEE Open J. Commun. Soc.*, vol. 3, pp. 2162–2177, 2022.
- [256] Z. Xiao, J. Yang, T. Mao, C. Xu, R. Zhang, Z. Han, and X.-G. Xia, "LEO satellite access network (LEO-SAN) towards 6G: Challenges and approaches," *IEEE Wireless Commun.*, vol. 31, no. 2, pp. 89–96, 2024.